Filter-Based Intelligent Output-Constrained Control of Uncertain MIMO Nonlinear Systems With Sensor and Actuator Faults

Ning Zhou, *Member, IEEE*, Canyang Zhao, Xiaodong Cheng, *Senior Member, IEEE*, and Yuanqing Xia, *Fellow, IEEE*

***Abstract*—This article studies the tracking problem for a class of strict-feedback uncertain multi-input–multi-output (MIMO) nonlinear systems, considering both the output constraints and multiple sensor/actuator faults. A novel control approach, named adaptive-neural-backstepping fault-tolerant constrained (ANBFTC) algorithm, is proposed, which incorporates the dynamic surface analysis into the iterative design. A filter-based adaptation coordinate transformation (FBACT) is introduced to define new backstepping iteration variables, eliminating the need for fault amplitudes and bias information. To further address the nonlinear uncertainties inherent in the system, we employ a learning approach, specifically utilizing radial basis function neural networks (RBFNNs), to approximate the uncertainty dynamics. This methodology not only mitigates the computational challenges typically associated with high-order derivatives in iterative designs but also ensures the convergence of tracking errors while adhering to output constraints, even in the presence of multiple sensor/actuator faults. Finally, numerical simulation results are presented to demonstrate the feasibility of the ANBFTC approach.**

***Index Terms*—Adaptation mechanism, coordinate transformation, filter-based adaptation, intelligent constraint control, multiple sensor and actuator faults.**

I. Introduction

IN RECENT decades, the tracking control problem of complex uncertain nonlinear systems has attracted considerable attention [1], [2], [3], [4], [5]. These systems find diverse applications in agricultural machinery [6], quadcopter vehicles [7], flexible manipulators [8], and surface vessel systems [9], etc. However, there are still many challenges to be addressed. For instance, due to harsh external conditions, equipment wear and aging, sensor and actuator faults inevitably occur during system operation. These faults lead to a decreased perception of system dynamics, resulting in degraded overall performance or potentially catastrophic consequences. Moreover, they also lead to increasing difficulties in control design. The other challenge is the constraints on system variables, stemming from physical limitations and safety requirements. For example, it is essential to constrain the position of a robotic arm to enable precise object manipulation along a specific path. While some control designs have used the concepts of barrier Lyapunov functions (BLFs) and nonlinear mappings, see [10], [11], [12], and [13], many of these approaches primarily focus on handling output and state constraints, neglecting faulty sensors/actuators. Therefore, how to design fault-tolerant tracking control while simultaneously satisfying asymmetric output constraints poses a challenging problem.

In the current literature, extensive studies have been focused on handling actuator faults, see [14], [15], [16], [17], [18], [19], [20], [21], [22], [23], [24], [25], [26], [27], [27], [28], [29], [30], [31] and the references therein. Various control schemes are presented for nonlinear systems with faulty actuators, including adaptive proportional and integral control [14], finite-time adaptive neural network (NN) control [15], [16], adaptive fuzzy control [22], prescribed performance control [17], [18], distributed adaptive fault-tolerant control (FTC) [19], adaptive event-triggered FTC [20], adaptive fault compensation methods [21], NNFTC [24], [25], [26], etc. Among them, multi-input–multi-output (MIMO) nonlinear systems are considered in [22], [25], and [26]. Furthermore, research works considering both actuator faults and output constraints or both actuator faults and state constraints can be found in [20], [22], [23], [27], [27], [28] and [29], [31], respectively.

On the other hand, faults in sensors appear to be another important factor affecting controller design, as serious sensor faults can reduce the reliability of states measurement and lead to system performance decline or even collapse. To overcome this challenge, different methods have been developed, such as state observers [32], [33], [34], sliding mode observers [35], sensor fault compensators [32], [36], event-triggered adaptive control [37], and neuron adaptive control [38], etc. In [35], [36], [37], and [38], sensor faults are only considered as

Received 10 December 2024; accepted 6 April 2025. This work was supported in part by the Natural Science Foundation of Hebei Province under Grant F2022208007, Grant F2024203102, Grant F2024208002, and Grant F2024208025; in part by the Key Cultivation of Basic Research of Scientific Research Foundation of Education Department of Hebei Province under Grant JZX2023005; in part by the National Natural Science Foundation of China under Grant U24A6005 and Grant 62403183; and in part by the Central Government-Guided Local S&T Development Foundation of Hebei Province under Grant 236Z1910G. This article was recommended by Associate Editor Y.-P. Huang. *(Corresponding author: Xiaodong Cheng.)*

Ning Zhou and Canyang Zhao are with the School of Electrical Engineering, Hebei University of Science and Technology, Shijiazhuang 050018, China (e-mail: zhouning2010@gmail.com; zhaocy128@hotmail.com).

Xiaodong Cheng is with the Mathematical and Statistical Methods Group (Biometris), Wageningen University & Research, 6700 AA Wageningen, The Netherlands (e-mail: xiaodong.cheng@wur.nl).

Yuanqing Xia is with the School of Automation, Beijing Institute of Technology, Beijing 100081, China (e-mail: xia_yuanqing@bit.edu.cn).

Color versions of one or more figures in this article are available at https://doi.org/10.1109/TSMC.2025.3559694.

Digital Object Identifier 10.1109/TSMC.2025.3559694

bounded bias, which exclude the possible multiplicative faults. [39] takes into account multiple sensor faults and output constraints in MIMO pure-feedback systems, which assumes that the system outputs are only affected by bias faults. Time-varying sensor faults are addressed in [34], where the control scheme relies on known boundaries of fault coefficients and biases. This requires precise information regarding sensor faults, which may not always be feasible in practice. For the interconnected nonlinear systems discussed, an adaptive fault-tolerant approach was developed in [40] to address the problem arising from general output constraints and sensor faults.

Note that the aforementioned works only investigated either actuator faults or sensor faults. However, in practical devices, both kinds of faults may appear simultaneously [41]. In [42], the leader-following fault-tolerant consensus problem of uncertain second-order multiagent is addressed with simultaneous sensor/actuator faults and time-varying delays. In [43], [44] and [45], [46], four adaptive algorithms are proposed for high-order nonlinear systems and multiagent systems, respectively, subjected to faulty sensors/actuators. Nevertheless, none of them have considered output constraints, which is the major factor restricting overall system performance and prevalent in practical systems. To address this design challenge arising from output constraints while considering both types of faults, two different approaches have been proposed. For SISO nonlinear systems, an adaptive fuzzy state-constrained control method is studied in [47], utilizing nonlinear state-dependent mapping for output tracking, without considering uncertainties. For block-triangular MIMO uncertain nonlinear systems, an event-triggered adaptive output-constrained control method is presented in [48], which requires the nonlinearity of the system to be locally Lipschitz continuous. Both methods rely on a single scalar adaptive parameter in each iteration step to handle overall nonlinearities and uncertainties. However, without assuming the locally Lipschitz property of the nonlinearities in the system, neither of the existing approaches in [47] and [48] can be applied to tackle the tracking control problem of uncertain MIMO nonlinear systems subject to output constraints and multiple sensor/actuator faults. So far, this problem remains largely underexplored, and no intelligent control methods have been proposed. This gap in the literature motivates the research presented in this article.

The proposed method is formulated using a modified backstepping framework via filter-based adaptation coordinate transformation (FBACT). Generally, the standard backstepping control leads to an "explosion of complexity" as system order increases, primarily due to the derivatives of virtual control variables. To mitigate this issue, we adopt the dynamic surface control (DSC) technique, following [49], which filters the synthesized virtual control variables at each iteration step. Furthermore, an radial basis function NN (RBFNN) is used to approximate the unknown nonlinear function, removing the requirement for it to be locally Lipschitz. Furthermore, a set of parameters is designed and estimated to account for NN optimal weights, sensor compresses faults, actuator gain variations, disturbances, etc. Overall, the main contributions are summarized as follows.

TABLE I
ORIGINAL TEXTS AND ABBREVIATIONS

Abbreviations	Meaning
ANBFTC	Adaptive-neural-backstepping fault-tolerant constraints
FBACT	Filter-based adaptation coordinate transformation
RBFNNs	Radial basis function neural networks
SGUUB	Semi-globally uniformly ultimately bounded
FTC	Fault-tolerant control
NNFTC	Neural-network fault-tolerant control
BLF	Barrier Lyapunov function
DSC	Dynamic surface control

1) A new adaptive-neural-backstepping fault-tolerant constrained (ANBFTC) algorithm is presented, capable of addressing general uncertain nonlinearities without assuming the locally Lipschitz property. The method can handle the tracking problem of a class of strict-feedback uncertain MIMO nonlinear systems with multiple sensors/actuators faults and time-varying asymmetric output constraints.
2) Considering sensor/actuator faults, a new FBACT is constructed by leveraging the DSC method and intelligent control technologies to generate iteration variables for the backstepping design, so that the a priori amplitudes and biases information of faults are not required, different from [39].
3) To address time-varying asymmetric constraints, the ANBFTC algorithm is delicately designed under the framework of BLFs with adaptation mechanism, and theoretical and simulation analysis are provided to show the convergence of all closed-loop signals.

The remainder is organized as follows. Section II states the essential knowledge and overall control objective. In Section III, the developed control mechanism and main results are expounded, while the main theorem is proven in Section IV. Sections V and VI provide a simulation example and conclude this article.

Notations: We denote $\mathbb{R}$ as the set of real numbers and $\mathbb{R}^n$ as the set of n-dimension real vectors. For a vector/matrix, $\|\cdot\|$ represents its Euclidean norm, and the ith order time derivative of any time-dependent variable v is denoted as $v^{(i)}$ with $i = 1, 2, \ldots, n$. Furthermore, sgn(v) denotes the sign function. Besides, for the sake of clarity, we provide the following list of abbreviations in Table I.

II. PRELIMINARIES AND PROBLEM FORMULATION

A. System Dynamics

Consider a class of fully interconnected strict-feedback uncertain MIMO nonlinear systems with the ith subsystem dynamics modeled by

$$\begin{aligned} \dot{x}_{i,j}(t) &= x_{i,j+1}(t) + f_{i,j}\left(\bar{x}_{N,j}\right) + d_{i,j}(t), \ \ i = 1, \ldots, N \\ \dot{x}_{i,n}(t) &= u_i(t) + f_{i,n}\left(\bar{x}_{N,n}\right) + d_{i,n}(t), \ \ j = 1, \ldots, n-1 \\ y_i(t) &= x_{i,1}(t) \end{aligned} \tag{1}$$

where $x_{i,k}(t) \in \mathbb{R}$, $k = 1, \ldots, n$ are states, $f_{i,k}(\bar{x}_{N,k})$:$\mathbb{R}^{Nk} \to \mathbb{R}$ are unknown but continuous nonlinear functions with $\bar{x}_{N,k} = [x_{1,1}(t), \ldots, x_{N,1}(t), \ldots, x_{1,k}(t), \ldots, x_{N,k}(t)]^T \in \mathbb{R}^{Nk}$,

and $y_i(t),\ u_i(t),\ d_{i,k}(t) \in \mathbb{R}$ are, respectively, the system output, control input, and external disturbances. The dynamics model of system (1) is derived from [2]. For simplicity, we set the control gain coefficient as 1. In practical terms, the time-varying asymmetric constraints

$$L_i(t) < y_i(t) < H_i(t),\ t \in [0, +\infty),\ i = 1, \ldots, N \tag{2}$$

should be satisfied, where $L_i(t)$ and $H_i(t)$ denote the lower and upper time-dependent constraint functions, respectively.

B. Modeling Sensor Faults and Actuator Faults

1) Assume that $x_{i,j}(t),\ j = 1, \ldots, n$ cannot be precisely measured, and the effectiveness of sensor j is described as [43]

$$x_{i,j}^f(t) \coloneqq \delta_{i,j} x_{i,j}(t) \text{ with } 0 < \delta_{i,j} \leq 1\ \forall t > t_{i,j}^f \tag{3}$$

where $\delta_{i,j}$ is the scaling factor. Using well-functioning sensing devices, the states $x_{i,j}$ are accurately measured as $x_{i,j}^f = x_{i,j}$. But if the sensor compresses faults occur at time $t_{i,j}^f > 0$ due to some unexpected circumstances, e.g., natural disasters, mechanical/physical faults, etc., the measurement may be compressed to (3).

2) Consider the ith subsystem subjecting to actuator faults modelled by [21]

$$u_i(t) \coloneqq \rho_i u_{ci}(t) + u_{ei}(t) \text{ with } 0 < \rho_i \leq 1\ \forall t > t_i^a \tag{4}$$

where ρ_i and $u_{ei}(t)$ are unknown actuator gain variation and actuator bias, respectively. When $\rho_i = 1$ and $u_{ei}(t) = 0$, it indicates that no fault/failure occurred. $t_i^a > 0$ represents the moment when the ith subsystem suffering actuator fault. $0 < \rho_i \leq 1$ means that the loss of actuator effectiveness is partial, and it is still operating such that u_i can be actuated by $u_{ci}(t)$ all the time.

C. Control Objectives

For $i = 1, \ldots, N$, $j = 1, \ldots, n$, the following assumptions regarding system (1) are required.

Assumption 1: There exists an unknown upper bound of the disturbance $\bar{d}_{i,j} \geq 0$ such that $|d_{i,j}(t)| \leq \bar{d}_{i,j}$ for all t.

Assumption 2: There exist unknown lower bounds on the scaling factors $\underline{\delta}_{i,j},\ \underline{\rho}_i > 0$ of the sensor and actuator faults such that $\underline{\delta}_{i,j} \leq \delta_{i,j} \leq 1$ and $\underline{\rho}_i \leq \rho_i \leq 1$.

Assumption 3 [15]: There exists an unknown upper bound on the bias of the actuator faults $\bar{u}_{ei} \geq 0$ such that $|u_{ei}(t)| \leq \bar{u}_{ei}$.

Remark 1: The constants $\bar{d}_{i,j}$, $\underline{\delta}_{i,j}$, $\underline{\rho}_i$, and $\bar{u}_{ei}$ in Assumptions 1–3 are unknown. Assumption 1 states that all environmental disturbances due to white noise, electromagnetic radiation, unknown load, harmonics, etc., are bounded. Assumption 2 shows that the state measurements are all partially available and the system remains fully actuated. Otherwise, if $\underline{\delta}_{i,j}$ and $\underline{\rho}_i$ are nonexistent, then the states become unobservable and the system is underactuated, in which case the output-based control scheme and active fault-tolerant mechanism should be considered, and that is out of our interest in this article. Assumption 3 describes that the additive faults u_{ei} of the actuator have an unknown upper bound, which reduces the conservative type of actuator fault model.

Let $y_{di}(t)$ be a desired trajectory for $y_i(t)$, which satisfies the following assumption.

Assumption 4 ([4], [50]): The signals $y_{di}(t)$ and $\dot{y}_{di}(t)$ are bounded in a compact set $\Omega_d \coloneqq \{y_{di}(t) | \underline{y}_{di} \leq y_{di}(t) \leq \bar{y}_{di},\ |\dot{y}_{di}(t)| \leq A_1,\ i = 1, \ldots, N\}$ with $L_i(t) < \underline{y}_{di}$ and $\bar{y}_{di} < H_i(t)$, where $A_1 > 0$ is unknown.

For system (1) with multiple faulty sensors and actuators, the overall objective is to construct a control strategy such that $y_i(t)$ can track $y_{di}(t)$ without breaking the constraints (2), and the tracking errors $z_{i,1}(t) \to \Omega_{z_{i,1}}$ as $t \to +\infty$ for $i = 1, \ldots, N$, where $z_{i,1}(t) \coloneqq x_{i,1}^f(t) - y_{di}(t)$, $\Omega_{z_{i,1}} \coloneqq \{z_{i,1}(t) | z_{i,1}(t) \in \mathbb{R},\ -\zeta_{Li} \leq z_{i,1}(t) \leq \zeta_{Hi}\}$.[1] Meanwhile, all signals are SGUUB and converge to the corresponding compact sets, as specified in Theorem 1.

To improve the readability and conciseness of this article, whenever applicable, we represent any function $F(*)$ with the variable $*$ as simply F.

III. Main Results and ANBFTC Control Design

In this section, a new fault-tolerant mechanism, i.e., the ANBFTC algorithm, is proposed for the time-varying asymmetric output constraints tracking problem, while addressing the design challenges arising from sensor/actuator faults.

A. Coordinate Transformations

The proposed controller is designed using a filter-based adaptation backstepping method. Since the standard backstepping approach cannot be directly applied to iterative design for system (1) with faulty sensors/actuators, we introduce an adaptation coordinate transformation of the ith subsystem as outlined below. Through this transformation, new variables $z_{i,j}$ are defined by incorporating the modeling of sensor/actuator faults, which are subsequently used for backstepping control design.

$$\begin{aligned} z_{i,1} &= x_{i,1} - y_{di},\ i = 1, \ldots, N \\ z_{i,j} &= x_{i,j} - \hat{v}_{i,j},\ j = 2, \ldots, n. \end{aligned} \tag{5}$$

To avoid the computational complexity explosion caused by high-order derivatives in backstepping design, we adopt the DSC technique [49] and designed a first-order filter as described in (6), where $\hat{v}_{i,j}$ is its output, and $v_{i,j-1}$ is a virtual controller.

$$\lambda_{i,j}\dot{\hat{v}}_{i,j} + \hat{v}_{i,j} = v_{i,j-1},\ j = 2, \ldots, n \tag{6}$$

with $\lambda_{i,j}$ a positive design parameter.

Define $e_{i,j}$ as the filter error variables given by

$$e_{i,j} \coloneqq \hat{v}_{i,j} - v_{i,j-1}. \tag{7}$$

From (3) and (5), since $\delta_{i,j}$ is unknown, $x_{i,j}$ and $z_{i,j}$ are also unknown, and thus the traditional coordinate transformations (5) is unusable for further design. To address this, first, we calculate $x_{i,j}$ from (3) as

$$x_{i,j} = \Delta_{i,j} x_{i,j}^f\ \forall\ t > t_{i,j}^f. \tag{8}$$

[1] We specify ζ_{Li} and ζ_{Hi} in (63) and (64).

where $\Delta_{i,j} \coloneqq 1/\delta_{i,j}$, and it is bounded with $1 \le 1/\delta_{i,j} \le 1/\underline{\delta}_{i,j}$ according to Assumption 2. Second, denote $\hat{\Delta}_{i,j}$ as the estimation of $\Delta_{i,j}$ and $\tilde{\Delta}_{i,j} \coloneqq \Delta_{i,j} - \hat{\Delta}_{i,j}$ as the estimation error. By extracting $x_{i,j}^f$ from $x_{i,j}$, (5) can be rewritten in a new FBACT form

$$\begin{aligned} z_{i,1} &= x_{i,1}^f - y_{di} \\ z_{i,j} &= \tilde{\Delta}_{i,j} x_{i,j}^f + \hat{z}_{i,j},\ j = 2, \ldots, n \\ \hat{z}_{i,j} &\coloneqq \hat{x}_{i,j} - \hat{v}_{i,j} \end{aligned} \tag{9}$$

where $\hat{x}_{i,j} \coloneqq \hat{\Delta}_{i,j} x_{i,j}^f$ is the estimation of $x_{i,j}$, and $x_{i,j}$ is rewritten as $x_{i,j} = \Delta_{i,j} x_{i,j}^f = \tilde{\Delta}_{i,j} x_{i,j}^f + \hat{\Delta}_{i,j} x_{i,j}^f$.

B. ANBFTC-Based Controller Design

To address the asymmetric output constraints problem of system (1), the tracking error $z_{i,1}$ should satisfy

$$\begin{aligned} -\xi_{Li} < z_{i,1} < \xi_{Hi},\ \ \xi_{Hi} \neq \xi_{Li} \\ -\xi_{Li}(0) < z_{i,1}(0) < \xi_{Hi}(0) \end{aligned}$$

where $\xi_{Hi} \coloneqq H_i - y_{di}$ and $\xi_{Li} \coloneqq y_{di} - L_i$ are two predefined smooth and positive time-dependent functions.

Then, we define an asymmetric BLF as follows:

$$V_{i,\phi} \coloneqq \frac{1}{2}\phi_i^2,\ \ \phi_i \coloneqq \frac{\xi_{Hi}\xi_{Li} z_{i,1}}{\left(\xi_{Hi} - z_{i,1}\right)\left(\xi_{Li} + z_{i,1}\right)}. \tag{10}$$

It shows that $\phi_i = 0$ if and only if $z_{i,1} = 0$. When $z_{i,1} \to \xi_{Hi}$, we have $\phi_i \to +\infty$, and when $z_{i,1} \to -\xi_{Li}$, we have $\phi_i \to -\infty$. Thus, for $-\xi_{Li} < z_{i,1} < \xi_{Hi}$, as long as ϕ_i is bounded, the output constraints will be guaranteed.

To facilitate the design of the controller, we take the time derivative of ϕ_i as

$$\dot{\phi}_i = w_i \dot{z}_{i,1} + o_i \dot{\xi}_{Hi} + h_i \dot{\xi}_{Li} \tag{11}$$

where

$$\begin{aligned} w_i &= \frac{\partial \phi_i}{\partial z_{i,1}} = \frac{\xi_{Hi}\xi_{Li}\left(z_{i,1}^2 + \xi_{Hi}\xi_{Li}\right)}{\left(\xi_{Hi} - z_{i,1}\right)^2\left(\xi_{Li} + z_{i,1}\right)^2} \\ o_i &= \frac{\partial \phi_i}{\partial \xi_{Hi}} = -\frac{\xi_{Li} z_{i,1}^2}{\left(\xi_{Hi} - z_{i,1}\right)^2\left(\xi_{Li} + z_{i,1}\right)} \\ h_i &= \frac{\partial \phi_i}{\partial \xi_{Li}} = \frac{\xi_{Hi} z_{i,1}^2}{\left(\xi_{Hi} - z_{i,1}\right)\left(\xi_{Li} + z_{i,1}\right)^2}. \end{aligned}$$

Consider the sensor faults, actuator faults, and time-varying asymmetric output constraints on system (1). The ANBFTC control scheme is iteratively designed for each subsystem.

Step 1: Design the virtual controller $v_{i,1}$ as

$$v_{i,1} = -\frac{1}{w_i}\hat{\Delta}_{i,1} s_{i,1} \tag{12}$$

$$\begin{aligned} s_{i,1} = \kappa_{i,1}\phi_i + o_i\dot{\xi}_{Hi} + h_i\dot{\xi}_{Li} + \frac{\hat{\psi}_{i,1}\phi_i w_i}{\sqrt{\phi_i^2 w_i^2 + \eta_{i,1}^2}} \\ + \hat{\theta}_i \phi_i w_i \|S_{i,1}(X_{i,1})\|^2 \end{aligned} \tag{13}$$

$$\dot{\hat{\psi}}_{i,1} = \frac{\beta_{i,1}\phi_i^2 w_i^2}{\sqrt{\phi_i^2 w_i^2 + \eta_{i,1}^2}} - \beta_{i,1}\varepsilon_{i,1}\hat{\psi}_{i,1} \tag{14}$$

$$\dot{\hat{\theta}}_i = \sigma_{i,1} w_i^2 \phi_i^2 \|S_{i,1}(X_{i,1})\|^2 - \sigma_{i,1}\tau_{i,1}\hat{\theta}_i \tag{15}$$

$$\dot{\hat{\Delta}}_{i,1} = \gamma_{i,1}\phi_{i,1} s_{i,1} - \gamma_{i,1}\hbar_{i,1}\hat{\Delta}_{i,1}. \tag{16}$$

where $\kappa_{i,1}$, $\sigma_{i,1}$, $\tau_{i,1}$, $\beta_{i,1}$, $\eta_{i,1}$, $\gamma_{i,1}$, $\hbar_{i,1}$, $\varepsilon_{i,1} > 0$ are design parameters. In (13), the variable $(1/w_i)$ offsets the coefficient of the first term in (11), and it collaborates with terms $o_i\dot{\xi}_{Hi}$ and $h_i\dot{\xi}_{Li}$ to offset the second and third terms in (11), while $\kappa_{i,1}$ denotes the control gain. $\hat{\theta}_i$ is the estimation of $\sup_{t\ge 0}\|W_{i,1}^{*\top}\|^2$. $W_{i,1}^{*\top}$ is NN optimal weight in (32), which addresses the nonlinear function $f_{i,1}(\bar{x}_{N,1})$ and the constraint function ϕ_i. $\hat{\psi}_{i,1}$ is the estimation of $\psi_{i,1}$ in (34), which addresses the external disturbance $d_{i,1}$ and approximation error $\epsilon_{i,1}$ in (32). $S_{i,1}(X_{i,1})$ (with $X_{i,1} \coloneqq [\bar{x}_{N,1}^{f\top}, y_{di}, \dot{y}_{di}, \xi_{Hi}, \xi_{Li}]^\top$) is the basis function of RBFNNs.

Step k ($2 \le k \le n-1$): Design the virtual controller $v_{i,k}$ as

$$\begin{aligned} v_{i,k} = -\kappa_{i,k}\hat{z}_{i,k} - \hat{W}_{i,k}^\top S_{i,k}(X_{i,k}) - \varsigma_{i,k} + \dot{\hat{v}}_{i,k} \\ - \frac{\hat{\psi}_{i,k}\hat{z}_{i,k}}{\sqrt{\hat{z}_{i,k}^2 + \eta_{i,k}^2}} \end{aligned} \tag{17}$$

$$\dot{\hat{\psi}}_{i,k} = \frac{\beta_{i,k}\hat{z}_{i,k}^2}{\sqrt{\hat{z}_{i,k}^2 + \eta_{i,k}^2}} - \beta_{i,k}\varepsilon_{i,k}\hat{\psi}_{i,k} \tag{18}$$

$$\dot{\hat{W}}_{i,k} = \sigma_{i,k}\hat{z}_{i,k} S_{i,k}(X_{i,k}) - \sigma_{i,k}\tau_{i,k}\hat{W}_{i,k} \tag{19}$$

$$\dot{\hat{\Delta}}_{i,k} = \max\{0,\ \gamma_{i,k} O_{i,k}\left(x_{i,k}^f\right)^2 - \gamma_{i,k}\hbar_{i,k}\hat{\Delta}_{i,k}\} \tag{20}$$

where $\kappa_{i,k}$, $\sigma_{i,k}$, $\tau_{i,k}$, $\beta_{i,k}$, $\varepsilon_{i,k}$, $\gamma_{i,k}$, $\eta_{i,k}$, and $\hbar_{i,k}$ are positive parameters to be designed. The function $\varsigma_{i,k}$ in $v_{i,k}$ is used to offset the residual term $z_{i,2}, \ldots, z_{i,n-2}$ generated in the previous step, while $\kappa_{i,k}$ denotes the control gain. $\hat{W}_{i,k}$ is the estimation of NN optimal weight $W_{i,k}^*$ in (41), which addresses the nonlinear function $f_{i,k}(\bar{x}_{N,k})$ and $\hat{v}_{i,k}$. $\hat{\psi}_{i,k}$ is the estimation of $\psi_{i,k}$ in (42), which addresses $d_{i,k}$ and $\epsilon_{i,k}$ in (41). $\hat{\Delta}_{i,k}$ estimates $\Delta_{i,k}$ in (8), which addresses the reciprocal of sensor multiplicative fault $\delta_{i,k}$. $S_{i,k}(X_{i,k})$ (with $X_{i,k} \coloneqq [\bar{x}_{N,1}^{f\top}, \hat{\bar{x}}_{N,k}^\top]^\top$) is the basis function of RBFNNs, where

$$\hat{\bar{x}}_{N,k} \coloneqq \left[\hat{x}_{1,2}, \ldots, \hat{x}_{N,2}, \ldots, \hat{x}_{1,k}, \ldots, \hat{x}_{N,k}\right]^\top.$$

For $k = 2$, $\varsigma_{i,k} = (1/2)\hat{z}_{i,k}$, $O_{i,k} = \alpha_{i,k}((\kappa_{i,k} + (1/2))\hat{z}_{i,k})^2 + (1/2)S_{i,k}^\top(X_{i,k})S_{i,k}(X_{i,k}) + (3/2) + \kappa_{i,k} + \alpha_{i,k}(([\hat{\psi}_{i,k}\hat{z}_{i,k}]/[\sqrt{\hat{z}_{i,k}^2+\eta_{i,k}^2}]))^2$, and $\alpha_{i,k} > 0$. For $k = 3, \ldots, n-1$, $\varsigma_{i,k} = \hat{z}_{i,k-1}$, $O_{i,k} = 1 + \kappa_{i,k} + \alpha_{i,k}(\kappa_{i,k}\hat{z}_{i,k})^2 + (1/2)S_{i,k}^\top(X_{i,k})S_{i,k}(X_{i,k}) + \alpha_{i,k}(([\hat{\psi}_{i,k}\hat{z}_{i,k}]/[\sqrt{\hat{z}_{i,k}^2+\eta_{i,k}^2}]))^2$.

Step n: Design the actual controller u_{ci} as

$$u_{ci} = -\hat{\varrho}_i s_i, \quad \text{with} \tag{21}$$

$$\dot{\hat{\varrho}}_i = \iota_i \hat{z}_{i,n} s_i - \iota_i \mu_i \hat{\varrho}_i \tag{22}$$

$$\begin{aligned} s_i = \kappa_{i,n}\hat{z}_{i,n} + \hat{z}_{i,n-1} - \dot{\hat{v}}_n + \frac{\hat{\psi}_{i,n}\hat{z}_{i,n}}{\sqrt{\hat{z}_{i,n}^2 + \eta_{i,n}^2}} \\ + \hat{W}_{i,n}^\top S_{i,n}(X_{i,n}) \end{aligned} \tag{23}$$

$$\dot{\hat{\psi}}_{i,n} = \frac{\beta_{i,n}\hat{z}_{i,n}^2}{\sqrt{\hat{z}_{i,n}^2 + \eta_{i,n}^2}} - \beta_{i,n}\varepsilon_{i,n}\hat{\psi}_{i,n} \tag{24}$$

$$\dot{\hat{W}}_{i,n} = \sigma_{i,n}\hat{z}_{i,n} S_{i,n}(X_{i,n}) - \sigma_{i,n}\tau_{i,n}\hat{W}_{i,n} \tag{25}$$

TABLE II
LIST OF ADAPTIVE DESIGN PARAMETERS

Adaptive Parameters	Design Function
$\hat{\theta}_i$, $i=1,\ldots,N$	Estimation of $\sup_{t\geq 0}\|W_{i,1}^*\|^2$.
$\hat{\psi}_{i,j}, j=1,\ldots,n$	Estimation of $\psi_{i,j}$ with $\psi_{i,j}:=\sup_{t\geq 0}\|\varphi_{i,j}\|$, $\varphi_{i,j}:=d_{i,j}+\epsilon_{i,j}$, where $d_{i,j}$ is the external disturbance, $\epsilon_{i,j}$ is the NN approximation error.
$\hat{\Delta}_{i,j}$	Estimation of $\Delta_{i,j}$ with $\Delta_{i,j}:=1/\delta_{i,j}$.
$\hat{W}_{i,k}, k=2,\ldots n$	Estimation of NN optimal weight $W_{i,k}^*$.
$\hat{\varrho}_i$	Estimation of ϱ_i with $\varrho_i:=1/\rho_i$ and ρ_i the actuator fault coefficient.

$$\dot{\hat{\Delta}}_{i,n}=\max\{0,\gamma_{i,n}O_{i,n}\left(x_{i,n}^f\right)^2-\gamma_{i,n}\hbar_{i,n}\hat{\Delta}_{i,n}\} \tag{26}$$

where $\kappa_{i,n}$, $\sigma_{i,n}$, $\tau_{i,n}$, $\beta_{i,n}$, $\varepsilon_{i,n}$, $\gamma_{i,n}$, $\hbar_{i,n}$, ι_i, $\eta_{i,n}$, and μ_i are the design positive parameters. $\hat{W}_{i,n}$ represents the estimated ideal weight $W_{i,n}^*$ for the NN in (51), which addresses the nonlinear function $f_{i,n}(\bar{x}_{N,n})$ and the filter output $\hat{\dot{v}}_{i,n}$. $\hat{\psi}_{i,n}$ estimates $\psi_{i,n}$ in (52), which addresses the external disturbance $d_{i,n}$, approximation error $\epsilon_{i,n}$ in (51), and actuator bias fault u_{ei}. $\hat{\Delta}_{i,n}$ estimates $\Delta_{i,n}$ in (8), which addresses the reciprocal of sensor multiplicative fault $\delta_{i,n}$. $\hat{\varrho}_i$ is the estimation of ϱ_i in (52), which addresses the reciprocal of actuator gain ρ_i. The intermediate variable s_i is designed to offset the residual term $z_{i,n-1}$ from the previous step and further prove the practical exponential convergence of $z_{i,n}$ in (54d), (54d), and (61). Then, by combining with $\hat{\varrho}_i$, the actual controller u_{ci} is obtained by compensation for the effect of the actuator gain. $S_{i,n}(X_{i,n})$ (with $X_{i,n}:=[\bar{x}_{N,1}^{f\top},\hat{\bar{x}}_{N,n}^{\top}]^{\top}$) denotes the basis function of RBFNNs, where

$$\hat{\bar{x}}_{N,n}:=\left[\hat{x}_{1,2},\ldots,\hat{x}_{N,2},\ldots,\hat{x}_{1,n},\ldots,\hat{x}_{N,n}\right]^{\top}.$$

In (26), $O_{i,n}:=(1/2)+\kappa_{i,n}+\alpha_{i,n}(\kappa_{i,n}\hat{z}_{i,n})^2+(1/2)s_i^2+\alpha_{i,n}((\hat{z}_{i,n}\hat{\psi}_{i,n}/\sqrt{\hat{z}_{i,n}^2+\eta_{i,n}^2}))^2+(1/2)S_{i,n}^{\top}(X_{i,n})S_{i,n}(X_{i,n})$ with $\alpha_{i,n}>0$.

The overall control strategy diagram is illustrated in Fig. 1, where all the adaptive design parameters are listed in Table II.

Remark 2: From the adaptation laws of $\hat{\Delta}_{i,k}$, $k=2,\ldots,n$, in (20) and (26), it is clear that $\dot{\hat{\Delta}}_{i,k}\geq 0$, and $\lim_{t\to\infty}\hat{\Delta}_{i,k}=\Delta_{i,j}$. Thus, $\tilde{\Delta}_{i,k}>0$, $\operatorname{sgn}(\tilde{\Delta}_{i,k})=1$ only if $\hat{\Delta}_{i,k}(0)<\Delta_{i,k}$. Since $\inf_{t\geq 0}\Delta_{i,k}=1$ from the definition $\Delta_{i,k}:=1/\delta_{i,k}$ with $0<\delta_{i,k}\leq 1$, we conclude that $\hat{\Delta}_{i,k}(0)\leq 1$. Some related elaborations can be found in [43, Remark 2].

C. Main Results of the ANBFTC Algorithm

Using controller (23) for system (1), we conclude that:

Theorem 1: Consider the system (1) with external disturbances, output constraints (2) and multiple sensor/actuator faults as described in (3) and (4). Let Assumptions 1–4 hold. By applying the ANBFTC scheme in (13)–(26) to system (1), for the Lyapunov function V in (58) with $V(0)\leq p$ and any given $p>0$, the following results are obtained.

(a) The transformed output tracking errors ϕ_i, the coordinate transformation errors $z_{i,k}$, the adaptive estimation errors $\tilde{W}_{i,k}$, $\tilde{\Delta}_{i,j}$, $\tilde{\psi}_{i,j}$, $\tilde{\theta}_i$, $\tilde{\varrho}_i$, and the first-order filter estimation errors $e_{i,k}$ converge to the sets Ω_{ϕ_i}, $\Omega_{z_{i,k}}$, $\Omega_{W_{i,k}}$, $\Omega_{\Delta_{i,j}}$, $\Omega_{\psi_{i,j}}$, Ω_{θ_i}, Ω_{ϱ_i}, and $\Omega_{e_{i,k}}$, respectively, as $t\to\infty$, where the sets are defined as follows:

$$\Omega_{\phi_i}:=\left\{\phi_i|\phi_i\in\mathbb{R},\ |\phi_i|\leq\sqrt{\frac{2C_2}{C_1}}\right\},\ i=1,\ldots,N$$

$$\Omega_{z_{i,k}}:=\left\{z_{i,k}|z_{i,k}\in\mathbb{R},\ |z_{i,k}|\leq\sqrt{\frac{2C_2}{C_1}}\right\},\ k=2,\ldots,n$$

$$\Omega_{W_{i,k}}:=\left\{\tilde{W}_{i,k}|\tilde{W}_{i,k}\in\mathbb{R},\ |\tilde{W}_{i,k}|\leq\sqrt{\frac{2\sigma_{i,k}C_2}{C_1}}\right\}$$

$$\Omega_{\Delta_{i,1}}:=\left\{\tilde{\Delta}_{i,1}|\tilde{\Delta}_{i,1}\in\mathbb{R},\|\tilde{\Delta}_{i,1}\|\leq\sqrt{\frac{2\gamma_{i,1}C_2}{\delta_{i,1}C_1}}\right\}$$

$$\Omega_{\Delta_{i,k}}:=\left\{\tilde{\Delta}_{i,k}|\tilde{\Delta}_{i,k}\in\mathbb{R},\ |\tilde{\Delta}_{i,k}|\leq\sqrt[3]{\frac{3\gamma_{i,k}C_2}{C_1}}\right\}$$

$$\Omega_{\psi_{i,j}}:=\left\{\tilde{\psi}_{i,j}|\tilde{\psi}_{i,j}\in\mathbb{R},\ |\tilde{\psi}_{i,j}|\leq\sqrt{\frac{2\beta_{i,j}C_2}{C_1}}\right\},\ j=1,\ldots,n$$

$$\Omega_{\theta_i}:=\left\{\tilde{\theta}_i|\tilde{\theta}_i\in\mathbb{R},\|\tilde{\theta}_i\|\leq\sqrt{\frac{2\sigma_{i,1}C_2}{C_1}}\right\}$$

$$\Omega_{\varrho_i}:=\left\{\tilde{\varrho}_i|\tilde{\varrho}_i\in\mathbb{R},\ |\tilde{\varrho}_i|\leq\sqrt{\frac{2\iota_iC_2}{\rho_iC_1}}\right\}$$

$$\Omega_{e_{i,k}}:=\left\{e_{i,k}|e_{i,k}\in\mathbb{R},\ |e_{i,k}|\leq\sqrt{\frac{2C_2}{C_1}}\right\}$$

with C_1 and C_2 defined in (60).

(b) Irrespective of the presence of sensor and actuator faults, y_i can track y_{di}, and $z_{i,1}\to\Omega_{z_{i,1}}$ as $t\to\infty$ with $\Omega_{z_{i,1}}:=\{z_{i,1}|z_{i,1}\in\mathbb{R},\ -\zeta_{Li}\leq z_{i,1}\leq\zeta_{Hi}\}$, ζ_{Li} and ζ_{Hi} defined in (63) and (64), shown at the bottom of p. 9 for $i=1,\ldots,N$.

(c) All signals are SGUUB.

(d) The output constraints (2) are satisfied.

IV. PROOF OF THEOREM 1

The proof is outlined in four steps (a), (b), (c), and (d), corresponding to the four main results in Theorem 1, respectively. Before moving forward, we provide two necessary lemmas.

Lemma 1 [11]: $\forall\ a,\ b\in\mathbb{R}$, $ab\leq(\varsigma^m/m)|a|^m+(1/n\varsigma^n)|b|^n$ holds with $(m-1)(n-1)=1$, $\varsigma>0$ and $m,n>1$.

Lemma 2 [17]: $\forall\ \eta(t)>0$, $z\in\mathbb{R}$

$$0\leq|z|-\frac{z^2}{\sqrt{z^2+\eta(t)^2}}<\eta(t)\ \text{holds.}$$

A. Proof of Theorem 1 (a)

For the ith subsystem, the proof is presented using the backstepping technique, which is divided into n steps.

Step 1: Combining (10), we define the Lyapunov candidate

$$V_{i,1}:=V_{i,\phi}+\frac{1}{2\sigma_{i,1}}\tilde{\theta}_i^2+\frac{1}{2\beta_{i,1}}\tilde{\psi}_{i,1}^2+\frac{1}{2}e_{i,2}^2+\frac{\delta_{i,1}}{2\gamma_{i,1}}\tilde{\Delta}_{i,1}^2 \tag{27}$$

where $\tilde{\theta}_i=\theta_i-\hat{\theta}_i$, $\tilde{\psi}_{i,1}=\psi_{i,1}-\hat{\psi}_{i,1}$.

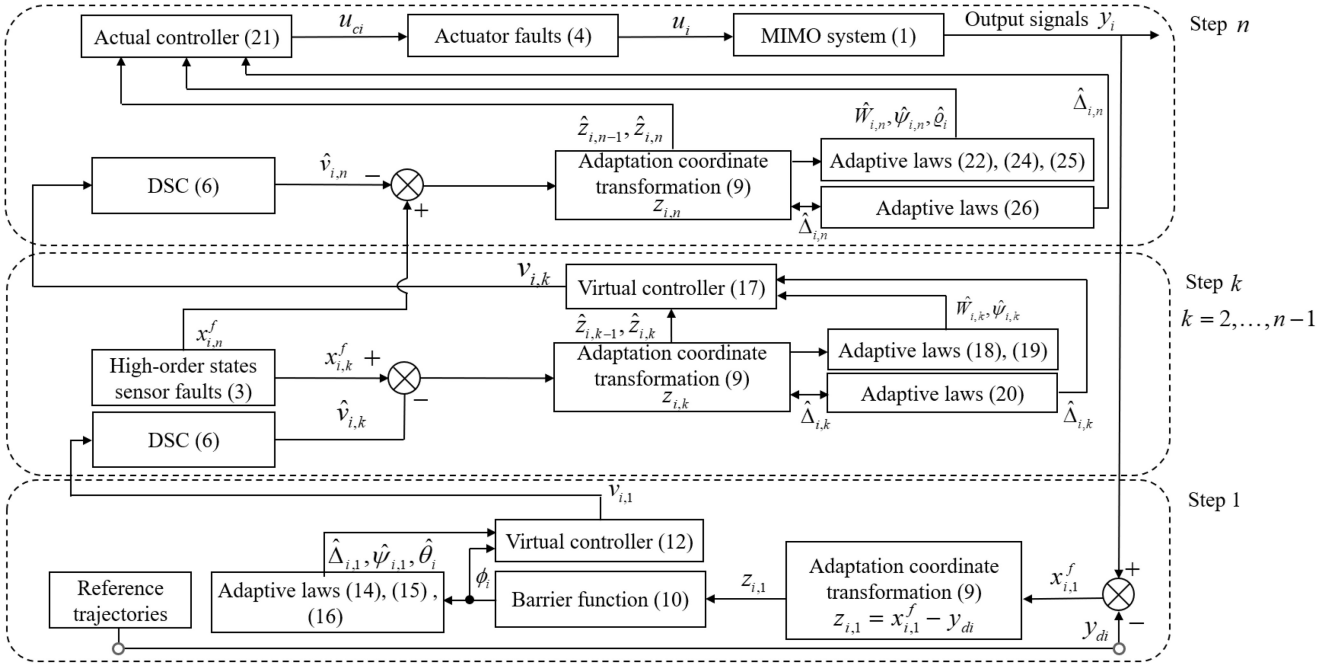

Fig. 1. Block Diagram of the ANBFTC Approach

Taking the derivative of $V_{i,1}$ yields

$$\dot{V}_{i,1} = \phi_i\dot{\phi}_i - \frac{\tilde{\theta}_i\dot{\hat{\theta}}_i}{\sigma_{i,1}} - \frac{\tilde{\psi}_{i,1}\dot{\hat{\psi}}_{i,1}}{\beta_{i,1}} + e_{i,2}\dot{e}_{i,2} - \frac{\delta_{i,1}}{\gamma_{i,1}}\tilde{\Delta}_{i,1}\dot{\hat{\Delta}}_{i,1}. \tag{28}$$

According to (1), (5), (7), and (11), we have

$$\begin{aligned}\phi_i\dot{\phi}_i &= \phi_i\big(w_i\dot{z}_{i,1} + o_i\dot{\xi}_{Hi} + h_i\dot{\xi}_{Li}\big)\\ &= \phi_i w_i\delta_{i,1}\big(z_{i,2} + e_{i,2} + v_{i,1} + f_{i,1}\big(\bar{x}_{N,1}\big) + d_{i,1}\big)\\ &\quad -\phi_i w_i\dot{y}_{di} + \phi_i\big(o_i\dot{\xi}_{Hi} + h_i\dot{\xi}_{Li}\big).\end{aligned} \tag{29}$$

By using Lemma 1, we obtain

$$\phi_i w_i\delta_{i,1}z_{i,2} \le \frac{1}{2}\phi_i^2 w_i^2\delta_{i,1}^2 + \frac{1}{2}z_{i,2}^2 \tag{30a}$$

$$\phi_i w_i\delta_{i,1}e_{i,2} \le \frac{1}{2}\phi_i^2 w_i^2\delta_{i,1}^2 + \frac{1}{2}e_{i,2}^2. \tag{30b}$$

Substituting (30) into (29), we obtain

$$\begin{aligned}\phi_i\dot{\phi}_i \le{}& \phi_i w_i\delta_{i,1}\big(v_{i,1} + d_{i,1}\big) + \frac{1}{2}e_{i,2}^2 + \frac{1}{2}z_{i,2}^2\\ &+\phi_i\big(o_i\dot{\xi}_{Hi} + h_i\dot{\xi}_{Li}\big) + \phi_i w_i\delta_{i,1}f_{i,1}\big(X_{i,1}\big)\end{aligned} \tag{31}$$

where $f_{i,1}(X_{i,1}) = \phi_i w_i\delta_{i,1} + f_{i,1}(\bar{x}_{N,1}) - \dot{y}_{di}/\delta_{i,1}$.

Applying the RBFNNs, any continuous function $f(X) : \mathbb{R}^l \to \mathbb{R}^m$ can be approximated using $W^* \in \mathbb{R}^{h\times m}$ and a basis function $S(X) : \mathbb{R}^l \to \mathbb{R}^h$ with h the number of NN nodes, $S_\iota(X) \coloneqq \exp[-(X-\chi_\iota)^\top(X-\chi_\iota)/(2b_\iota^2)]$ for $\iota = 1,\ldots,h$, $\chi_\iota \in \mathbb{R}^l$ represents the center and $b_\iota \in \mathbb{R}$ represents the width. Furthermore $\forall\ \bar{\epsilon} > 0$, there exists $\Omega_X \subset \mathbb{R}^l$ such that

$$f(X) = W^{*\top}S(X) + \epsilon(X) \text{ with } \|\epsilon(\cdot)\| \le \bar{\epsilon}\ \forall X \in \Omega_X.$$

Let $l = N+4$ and $m = 1$ for function $f_{i,1}(X_{i,1})$ approximation. By using vector $W_{i,1}^* \in \mathbb{R}^h$, for any $\bar{\epsilon}_{i,1} > 0$, there exist $\Omega_{X_{i,1}} \in \mathbb{R}^{N+4}$ and $S_{i,1} : \mathbb{R}^{N+4} \to \mathbb{R}^h$, such that $f_{i,1}(X_{i,1})$ is described as

$$f_{i,1}\big(X_{i,1}\big) = W_{i,1}^{*\top}S_{i,1}\big(X_{i,1}\big) + \epsilon_{i,1}\big(X_{i,1}\big) \tag{32}$$

with $|\epsilon_{i,1}(X_{i,1})| \le \bar{\epsilon}_{i,1}$ and $\bar{\epsilon}_{i,1} \ge 0$.

From Lemma 1, it yields

$$\phi_i w_i\delta_{i,1}W_{i,1}^*S_{i,1}\big(X_{i,1}\big) \le \theta_i w_i^2\phi_i^2\|S_{i,1}\big(X_{i,1}\big)\|^2 + \frac{1}{4} \tag{33}$$

where $\theta_i \coloneqq \sup_{t\ge 0}\|W_{i,1}^*\|^2$.

Define $\varphi_{i,1} \coloneqq d_{i,1} + \epsilon_{i,1}$. From Lemma 2, it yields

$$\phi_i w_i\delta_{i,1}\varphi_{i,1} \le \frac{\psi_{i,1}\phi_i^2 w_i^2}{\sqrt{\phi_i^2 w_i^2 + \eta_{i,1}^2}} + \psi_{i,1}\eta_{i,1} \tag{34}$$

with $\psi_{i,1} \coloneqq \sup_{t\ge 0}|\varphi_{i,1}|$.

From (6), (7), and Lemma 1, we further have

$$e_{i,2}\dot{e}_{i,2} = e_{i,2}\left(-\frac{e_{i,2}}{\lambda_{i,2}} - \dot{v}_{i,1}\right) \le \left(\frac{1}{4} - \frac{1}{\lambda_{i,2}}\right)e_{i,2}^2 + \Phi_{i,1}^2 \tag{35}$$

where $\Phi_{i,1} \coloneqq \dot{v}_{i,1}$.

Substituting (13)–(15) and (31)–(35) into (28) yields

$$\begin{aligned}\dot{V}_{i,1} \le{}& -\kappa_{i,1}\phi_i^2 - \varpi_{i,2}e_{i,2}^2 + \tau_{i,1}\tilde{\theta}_{i,1}\hat{\theta}_{i,1} + \varepsilon_{i,1}\tilde{\psi}_{i,1}\hat{\psi}_{i,1}\\ &+\frac{z_{i,2}^2}{2} + \Phi_{i,1}^2 + \psi_{i,1}\eta_{i,1} + \delta_{i,1}\hbar_{i,1}\tilde{\Delta}_{i,1}\hat{\Delta}_{i,1} + \frac{1}{4}\end{aligned} \tag{36}$$

where $(1/[\lambda_{i,2}]) - (3/4) \ge \varpi_{i,2}$ with $\varpi_{i,2} > 0$ represents a constant.

Step k ($2 \le k \le n-1$): Define the following Lyapunov candidate:

$$\begin{aligned}V_{i,k} \coloneqq{}& V_{i,k-1} + \frac{1}{2}z_{i,k}^2 + \frac{1}{2\sigma_{i,k}}\tilde{W}_{i,k}^\top\tilde{W}_{i,k} + \frac{1}{3\gamma_{i,k}}|\tilde{\Delta}_{i,k}|^3\\ &+\frac{1}{2\beta_{i,k}}\tilde{\psi}_{i,k}^2 + \frac{1}{2}e_{i,k+1}^2\end{aligned} \tag{37}$$

where $\tilde{W}_{i,k} \coloneqq W_{i,k}^* - \hat{W}_{i,k}$, $\tilde{\Delta}_{i,k} \coloneqq \Delta_{i,k} - \hat{\Delta}_{i,k}$, and $\tilde{\psi}_{i,k} \coloneqq \psi_{i,k} - \hat{\psi}_{i,k}$.

Differentiating $V_{i,k}$, we have

$$\dot{V}_{i,k} = \dot{V}_{i,k-1} - \frac{1}{\sigma_{i,k}}\tilde{W}_{i,k}^\top \dot{\hat{W}}_{i,k} - \frac{1}{\gamma_{i,k}}\tilde{\Delta}_{i,k}^2 \dot{\hat{\Delta}}_{i,k}\mathrm{sgn}\left(\tilde{\Delta}_{i,k}\right) - \frac{1}{\beta_{i,k}}\tilde{\psi}_{i,k}\dot{\hat{\psi}}_{i,k} + z_{i,k}\dot{z}_{i,k} + e_{i,k+1}\dot{e}_{i,k+1}. \tag{38}$$

Differentiating $V_{i,k-1}$ with respect to t, one has

$$\begin{aligned}\dot{V}_{i,k-1} \le & -\kappa_{i,1}\phi_i^2 - \sum_{j=2}^{k-1} K_{i,j} z_{i,j}^2 - \sum_{j=2}^{k} \varpi_{i,j} e_{i,j}^2 + \sum_{j=2}^{k-1}\frac{1}{2}\psi_{i,j}^2 \\ & + \sum_{j=1}^{k-1}\varepsilon_{i,j}\tilde{\psi}_{i,j}\hat{\psi}_{i,j} + \sum_{j=2}^{k-1}\hbar_{i,j}\tilde{\Delta}_{i,j}^2\hat{\Delta}_{i,j}\mathrm{sgn}\left(\tilde{\Delta}_{i,j}\right) \\ & + \sum_{j=2}^{k-1}\tau_{i,j}\tilde{W}_{i,j}^\top\hat{W}_{i,j} + \sum_{j=2}^{k-1}\frac{1}{2}\tilde{W}_{i,j}^\top\tilde{W}_{i,j} + \sum_{j=1}^{k-1}\Phi_{i,j}^2 \\ & + \sum_{j=1}^{k-1}\psi_{i,j}\eta_{i,j} + \tau_{i,1}\tilde{\theta}_i\hat{\theta}_i + \delta_{i,1}\hbar_{i,1}\tilde{\Delta}_{i,1}\hat{\Delta}_{i,1} \\ & + \Lambda_{i,k-1} + T_{i,k-1}. \end{aligned} \tag{39}$$

For $k = 2$, $\Lambda_{i,k-1} = (1/2)z_{i,k}^2$, $T_{i,k-1} = (1/4)$. For $k = 3, \ldots, n-1$, $\Lambda_{i,k-1} = -(1/2)(\tilde{\Delta}_{i,k-1}x_{i,k-1}^f)^2 + z_{i,k-1}z_{i,k}$, $T_{i,k-1} = (1/4) + \sum_{j=2}^{k-1}(1/[2\alpha_{i,j}])$, and $\alpha_{i,j} > 0$. $K_{i,j} \coloneqq \kappa_{i,j} - (1/2) > 0$ for $j = 2$, and $K_{i,j} \coloneqq \kappa_{i,j} - 1 > 0$ for $j = 3, \ldots, k-1$. $(1/[\lambda_{i,j}]) - (3/4) \ge \varpi_{i,j}$ $(j = 2, \ldots, k)$ with $\varpi_{i,j} > 0$ represents a constant.

From (1), (5), and (7), we have

$$z_{i,k}\dot{z}_{i,k} = z_{i,k}\left(z_{i,k+1} + e_{i,k+1} + v_{i,k} - \dot{\hat{v}}_{i,k} + f_{i,k}\left(X_{i,k}\right) + d_{i,k}\right) \tag{40}$$

where $f_{i,k}(X_{i,k}) = f_{i,k}(\bar{x}_{N,k})$. Following the design in (32), let $l = kN$. Then, we rewrite $f_{i,k}(X_{i,k})$ as

$$f_{i,k}\left(X_{i,k}\right) = W_{i,k}^{*\top} S_{i,k}\left(X_{i,k}\right) + \epsilon_{i,k}\left(X_{i,k}\right) \tag{41}$$

where $|\epsilon_{i,k}(X_{i,k})| \le \bar{\epsilon}_{i,k}$ with $\bar{\epsilon}_{i,k} \ge 0$.

Moreover, define

$$\varphi_{i,k} \coloneqq d_{i,k} + \epsilon_{i,k}. \tag{42}$$

Substituting (41) and (42) into (40) yields

$$z_{i,k}\dot{z}_{i,k} = z_{i,k}\left(z_{i,k+1} + e_{i,k+1} + v_{i,k} - \dot{\hat{v}}_{i,k} + W_{i,k}^{*\top} S_{i,k}\left(X_{i,k}\right) + \varphi_{i,k}\right). \tag{43}$$

By utilizing (9) and Lemmas 1 and 2, we have

$$z_{i,k}e_{i,k+1} \le \frac{1}{2}z_{i,k}^2 + \frac{1}{2}e_{i,k+1}^2 \tag{44a}$$

$$z_{i,k}\tilde{W}_{i,k}^\top S_{i,k}(X_{i,k}) \le \frac{1}{2}\left(\tilde{\Delta}_{i,k}x_{i,k}^f\right)^2 S_{i,k}^\top(X_{i,k})S_{i,k}(X_{i,k}) + \frac{1}{2}\tilde{W}_{i,k}^\top\tilde{W}_{i,k} + \hat{z}_{i,k}\tilde{W}_{i,k}^\top S_{i,k}(X_{i,k}) \tag{44b}$$

$$z_{i,k}\varphi_{i,k} \le \frac{\hat{z}_{i,k}^2\psi_{i,k}}{\sqrt{\hat{z}_{i,k}^2 + \eta_{i,k}^2}} + \psi_{i,k}\eta_{i,k} + \frac{1}{2}\left(\tilde{\Delta}_{i,k}x_{i,k}^f\right)^2 + \frac{1}{2}\psi_{i,k}^2 \tag{44c}$$

$$e_{i,k+1}\dot{e}_{i,k+1} \le \left(\frac{1}{4} - \frac{1}{\lambda_{i,k+1}}\right)e_{i,k+1}^2 + \Phi_{i,k}^2 \tag{44d}$$

$$-\frac{\hat{z}_{i,k}\hat{\psi}_{i,k}\tilde{\Delta}_{i,k}x_{i,k}^f}{\sqrt{\hat{z}_{i,k}^2 + \eta_{i,k}^2}} \le \frac{\alpha_{i,k}\left(\hat{\psi}_{i,k}\hat{z}_{i,k}\tilde{\Delta}_{i,k}x_{i,k}^f\right)^2}{\hat{z}_{i,k}^2 + \eta_{i,k}^2} + \frac{1}{4\alpha_{i,k}} \tag{44e}$$

where $\psi_{i,k} \coloneqq \sup_{t\ge 0}|\varphi_{i,k}|$, $\Phi_{i,k} \coloneqq \dot{v}_{i,k}$. For $k = 2$, we have

$$\begin{aligned} -\left(\kappa_{i,k} + \frac{1}{2}\right)z_{i,k}\hat{z}_{i,k} \le & \left(\kappa_{i,k} + \frac{1}{2}\right)\left(\tilde{\Delta}_{i,k}x_{i,k}^f\right)^2 + \frac{1}{4\alpha_{i,k}} \\ & + \alpha_{i,k}\left(\left(\kappa_{i,k} + \frac{1}{2}\right)\hat{z}_{i,k}\tilde{\Delta}_{i,k}x_{i,k}^f\right)^2 - \left(\kappa_{i,k} + \frac{1}{2}\right)z_{i,k}^2. \end{aligned} \tag{45}$$

For $k = 3, \ldots, n-1$, one has

$$\begin{aligned} -k_{i,k}z_{i,k}\ \hat{z}_{i,k} &= -k_{i,k}z_{i,k}\left(z_{i,k} - \tilde{\Delta}_{i,k}x_{i,k}^f\right) \\ &= -k_{i,k}z_{i,k}^2 + k_{i,k}\left(\hat{z}_{i,k} + \tilde{\Delta}_{i,k}x_{i,k}^f\right)\tilde{\Delta}_{i,k}x_{i,k}^f \\ &\le -k_{i,k}z_{i,k}^2 + k_{i,k}\left(\tilde{\Delta}_{i,k}x_{i,k}^f\right)^2 + \frac{1}{4a_{i,k}} \\ &\quad + a_{i,k}\left(k_{i,k}\hat{z}_{i,k}\tilde{\Delta}_{i,k}x_{i,k}^f\right)^2 \end{aligned} \tag{46a}$$

$$-z_{i,k}\hat{z}_{i,k-1} \le -z_{i,k}z_{i,k-1} + \frac{1}{2}z_{i,k}^2 + \frac{1}{2}\left(\tilde{\Delta}_{i,k-1}x_{i,k-1}^f\right)^2. \tag{46b}$$

Substituting (17)–(20), (39), and (43)–(46) into (38) yields

$$\begin{aligned}\dot{V}_{i,k} \le & -\kappa_{i,1}\phi_i^2 - \sum_{j=2}^{k} K_{i,j} z_{i,j}^2 - \sum_{j=2}^{k+1}\varpi_{i,j}e_{i,j}^2 + T_{i,k} \\ & + \sum_{j=1}^{k}\varepsilon_{i,j}\tilde{\psi}_{i,j}\hat{\psi}_{i,j} + \sum_{j=2}^{k}\hbar_{i,j}\tilde{\Delta}_{i,j}^2\hat{\Delta}_{i,j}\mathrm{sgn}\left(\tilde{\Delta}_{i,j}\right) \\ & + \sum_{j=2}^{k}\tau_{i,j}\tilde{W}_{i,j}^\top\hat{W}_{i,j} + \sum_{j=2}^{k}\frac{1}{2}\tilde{W}_{i,j}^\top\tilde{W}_{i,j} + \sum_{j=1}^{k}\Phi_{i,j}^2 \\ & + \sum_{j=1}^{k}\psi_{i,j}\eta_{i,j} + \sum_{j=2}^{k}\frac{1}{2}\psi_{i,j}^2 + \tau_{i,1}\tilde{\theta}_i\hat{\theta}_i \\ & + \delta_{i,1}\hbar_{i,1}\tilde{\Delta}_{i,1}\hat{\Delta}_{i,1} + \Lambda_{i,k}, \end{aligned} \tag{47}$$

where $\Lambda_{i,k} = z_{i,k}z_{i,k+1} - (1/2)(\tilde{\Delta}_{i,k}x_{i,k}^f)^2$, $T_{i,k} = (1/4) + \sum_{j=2}^{k}(1/[2\alpha_{i,j}])$, $\alpha_{i,j} > 0$. $K_{i,j} \coloneqq \kappa_{i,j} - (1/2) > 0$ for $j = 2$, and $K_{i,j} \coloneqq \kappa_{i,j} - 1 > 0$ for $j = 3, \ldots, k$. $(1/[\lambda_{i,j}]) - (3/4) \ge \varpi_{i,j}$ $(j = 2, \ldots, k+1)$ with $\varpi_{i,j} \ge 0$.

Step n: Define the following Lyapunov candidate:

$$\begin{aligned} V_{i,n} \coloneqq & V_{i,n-1} + \frac{1}{2}z_{i,n}^2 + \frac{1}{2\sigma_{i,n}}\tilde{W}_{i,n}^\top\tilde{W}_{i,n} \\ & + \frac{1}{3\gamma_{i,n}}|\tilde{\Delta}_{i,n}|^3 + \frac{1}{2\beta_{i,n}}\tilde{\psi}_{i,n}^2 + \frac{\rho_i}{2\iota_i}\tilde{\varrho}_i^2 \end{aligned} \tag{48}$$

where $\tilde{W}_{i,n} \coloneqq W_{i,n}^* - \hat{W}_{i,n}$, $\tilde{\Delta}_{i,n} \coloneqq \Delta_{i,n} - \hat{\Delta}_{i,n}$, $\tilde{\psi}_{i,n} \coloneqq \psi_{i,n} - \hat{\psi}_{i,n}$, and $\tilde{\varrho}_i \coloneqq \varrho_i - \hat{\varrho}_i$.

Differentiating $V_{i,n}$ with respect to t yields

$$\dot{V}_{i,n} = \dot{V}_{i,n-1} + z_{i,n}\dot{z}_{i,n} - \frac{1}{\gamma_{i,n}}\tilde{\Delta}_{i,n}^2\dot{\hat{\Delta}}_{i,n}\mathrm{sgn}\left(\tilde{\Delta}_{i,n}\right)$$

$$-\frac{1}{\sigma_{i,n}}\tilde{W}_{i,n}^{\top}\dot{\hat{W}}_{i,n}-\frac{1}{\beta_{i,n}}\tilde{\psi}_{i,n}\dot{\hat{\psi}}_{i,n}-\frac{\rho_i}{\iota_i}\tilde{\varrho}_i\dot{\hat{\varrho}}_i. \tag{49}$$

From (1), (4), and (5), it yields

$$\begin{aligned} z_{i,n}\dot{z}_{i,n}=z_{i,n}\big(&\rho_i u_{ci}+u_{ei}+d_{i,n}\\ &+f_{i,n}(X_{i,n})-\dot{\hat{\nu}}_{i,n}\big), \end{aligned} \tag{50}$$

where $f_{i,n}(X_{i,n})=f_{i,n}(x_{N,n})$. Following the design in (32), let $l=nN$ and $m=1$, we rewrite $f_{i,n}(X_{i,n})$ as

$$f_{i,n}(X_{i,n})=W_{i,n}^{*\top}S_{i,n}(X_{i,n})+\epsilon_{i,n} \tag{51}$$

where $|\epsilon_{i,n}|\le\bar{\epsilon}_{i,n}$ with $\bar{\epsilon}_{i,n}\ge 0$.

Moreover, let

$$\varrho_i:=1/\rho_i,\quad \varphi_{i,n}:=u_{ei}+d_{i,n}+\epsilon_{i,n}. \tag{52}$$

Substituting (51) and (52) into (50) yields

$$\begin{aligned} z_{i,n}\dot{z}_{i,n}=z_{i,n}\big(&\rho_i u_{ci}+W_{i,n}^{*\top}S_{i,n}(X_{i,n})\\ &+\varphi_{i,n}-\dot{\hat{\nu}}_{i,n}\big) \end{aligned} \tag{53}$$

By utilizing (9), Lemmas 1 and 2, we get

$$-\kappa_{i,n}z_{i,n}\hat{z}_{i,n}\le-\kappa_{i,n}z_{i,n}^2+\kappa_{i,n}\Big(\tilde{\Delta}_{i,n}x_{i,n}^f\Big)^2+\frac{1}{4\alpha_{i,n}}+\alpha_{i,n}\Big(\kappa_{i,n}\hat{z}_{i,n}\tilde{\Delta}_{i,n}x_{i,n}^f\Big)^2 \tag{54a}$$

$$-z_{i,n}\hat{z}_{i,n-1}\le-z_{i,n-1}z_{i,n}+\frac{1}{2}z_{i,n}^2+\frac{1}{2}\Big(\tilde{\Delta}_{i,n-1}x_{i,n-1}^f\Big)^2 \tag{54b}$$

$$z_{i,n}\tilde{W}_{i,n}^{\top}S_{i,n}(X_{i,n})\le\frac{1}{2}\Big(\tilde{\Delta}_{i,n}x_{i,n}^f\Big)^2S_{i,n}^{\top}(X_{i,n})S_{i,n}(X_{i,n})+\frac{1}{2}\tilde{W}_{i,n}^{\top}\tilde{W}_{i,n}+\hat{z}_{i,n}\tilde{W}_{i,n}^{\top}S_{i,n}(X_{i,n}) \tag{54c}$$

$$z_{i,n}\varphi_{i,n}\le\frac{\hat{z}_{i,n}^2\psi_{i,n}}{\sqrt{\hat{z}_{i,n}^2+\eta_{i,n}^2}}+\eta_{i,n}\psi_{i,n}+\frac{1}{2}\Big(\tilde{\Delta}_{i,n}x_{i,n}^f\Big)^2+\frac{\psi_{i,n}^2}{2} \tag{54d}$$

$$-\frac{\hat{z}_{i,n}\hat{\psi}_{i,n}\tilde{\Delta}_{i,n}x_{i,n}^f}{\sqrt{\hat{z}_{i,n}^2+\eta_{i,n}^2}}\le\frac{\alpha_{i,n}\Big(\hat{\psi}_{i,n}\hat{z}_{i,n}\tilde{\Delta}_{i,n}x_{i,n}^f\Big)^2}{\hat{z}_{i,n}^2+\eta_{i,n}^2}+\frac{1}{4\alpha_{i,n}}, \tag{54e}$$

where $\psi_{i,n}:=\sup_{t\ge0}|\varphi_{i,n}|$. Adding and subtracting $z_{i,n}s_i$ to (49), and substituting (23)–(26), (47), (53)–(56a) into (49), it yields

$$\begin{aligned} \dot{V}_{i,n}\le&-\kappa_{i,1}\phi_i^2-\sum_{j=2}^{n}\Big(K_{i,j}z_{i,j}^2+\varpi_{i,j}e_{i,j}^2\Big)+\sum_{j=1}^{n-1}\Phi_{i,j}^2\\ &+\sum_{j=2}^{n}\left(\tau_{i,j}\tilde{W}_{i,j}^{\top}\hat{W}_{i,j}+\frac{\tilde{W}_{i,j}^{\top}\tilde{W}_{i,j}}{2}+\hbar_{i,j}\tilde{\Delta}_{i,j}^2\hat{\Delta}_{i,j}\mathrm{sgn}(\tilde{\Delta}_{i,j})\right)\\ &+\sum_{j=1}^{n}(\varepsilon_{i,j}\tilde{\psi}_{i,j}\hat{\psi}_{i,j}+\psi_{i,j}\eta_{i,j}+\frac{1}{2}\psi_{i,j}^2+\tau_{i,1}\tilde{\theta}_i\hat{\theta}_i\\ &+\delta_{i,1}\hbar_{i,1}\tilde{\Delta}_{i,1}\hat{\Delta}_{i,1}-z_{i,n}\rho_i\hat{\varrho}_i s_i-\hat{z}_{i,n}\rho_i\tilde{\varrho}_i s_i+z_{i,n}s_i\\ &-\frac{1}{2}\Big(\tilde{\Delta}_{i,n}x_{i,n}^f s_i\Big)^2+\rho_i\mu_i\tilde{\varrho}_i\hat{\varrho}_i+\sum_{j=2}^{n}\frac{1}{2\alpha_{i,j}}+\frac{1}{4}. \end{aligned} \tag{55}$$

Using Lemma 1, one has ($j=1,\dots,n,\ k=2,\dots,n$)

$$\tilde{W}_{i,j}^{\top}\hat{W}_{i,j}\le\frac{1}{2}\Big(W_{i,j}^{\top}W_{i,j}^{*}-\tilde{W}_{i,j}^{\top}\tilde{W}_{i,j}\Big) \tag{56a}$$

$$\tilde{\Delta}_{i,k}^2\hat{\Delta}_{i,k}\mathrm{sgn}\Big(\tilde{\Delta}_{i,k}\Big)\le\frac{1}{3}\Big(\Delta_{i,k}^3-|\tilde{\Delta}_{i,k}|^3\Big) \tag{56b}$$

$$\tilde{\psi}_{i,j}\hat{\psi}_{i,j}\le\frac{1}{2}\psi_{i,j}^2-\frac{1}{2}\tilde{\psi}_{i,j}^2 \tag{56c}$$

$$\tilde{\varrho}_i\hat{\varrho}_i\le\frac{1}{2}\varrho_i^2-\frac{1}{2}\tilde{\varrho}_i^2 \tag{56d}$$

$$\begin{aligned} z_{i,n}s_i-\hat{z}_{i,n}\quad&\rho_i\tilde{\varrho}_i s_i-z_{i,n}\rho_i\hat{\varrho}_i s_i\\ &\le\frac{1}{2}\Big(\tilde{\Delta}_{i,n}x_{i,n}^f s_i\Big)^2+\frac{1}{2}(\rho_i\tilde{\varrho}_i)^2 \end{aligned} \tag{56e}$$

$$\tilde{\theta}_i\hat{\theta}_i\le\frac{1}{2}\theta_i^2-\frac{1}{2}\tilde{\theta}_i^2 \tag{56f}$$

$$\tilde{\Delta}_{i,1}\hat{\Delta}_{i,1}\le\frac{1}{2}\Delta_{i,1}^2-\frac{1}{2}\tilde{\Delta}_{i,1}^2 \tag{56g}$$

Substituting (56a) into (55), it yields

$$\begin{aligned} \dot{V}_{i,n}\le&-\kappa_{i,1}\phi_i^2-\sum_{j=2}^{n}\Big(K_{i,j}z_{i,j}^2+\varpi_{i,j}e_{i,j}^2\Big)-\sum_{j=1}^{n}\frac{\varepsilon_{i,j}}{2}\tilde{\psi}_{i,j}^2\\ &-\sum_{j=2}^{n}\Big(\frac{\tau_{i,j}-1}{2}\tilde{W}_{i,j}^{\top}\tilde{W}_{i,j}+\frac{\hbar_{i,j}}{3}|\tilde{\Delta}_{i,j}|^3\Big)+\sum_{j=1}^{n-1}\Phi_{i,j}^2\\ &-\frac{\tau_{i,1}}{2}\tilde{\theta}_{i,1}^2-\frac{\delta_{i,1}\hbar_{i,1}}{2}\tilde{\Delta}_{i,1}^2-\frac{1}{2}\rho_i(\mu_i-\rho_i)\tilde{\varrho}_i^2+\Pi_i. \end{aligned} \tag{57}$$

Let $\eta_{i,j}=a_{i,j}\exp(-b_{i,j}t)$, $a_{i,j}>0$, $b_{i,j}>0$, $|\eta_{i,j}|\le\bar{\eta}_{i,j}$, then $\Pi_i:=\sum_{j=1}^{n}(([\varepsilon_{i,j}]/2)\psi_{i,j}^2+\psi_{i,j}\bar{\eta}_{i,j})+\sum_{j=2}^{n}(([\tau_{i,j}]/2)W_{i,j}^{*\top}W_{i,j}^{*}+(1/2)\psi_{i,j}^2+([\hbar_{i,j}]/3)\Delta_{i,j}^3)+([\rho_i\mu_i]/2)\varrho_i^2+([\tau_{i,1}]/2)\theta_i^2+([\delta_{i,1}\hbar_{i,1}]/2)\Delta_{i,1}^2+T_{i,n}$ with $T_{i,n}:=(1/4)+\sum_{j=2}^{n}(1/2\alpha_{i,j})$ and $\alpha_{i,j}>0$. $K_{i,j}:=\kappa_{i,j}-(1/2)>0$ for $j=2$, and $K_{i,j}:=\kappa_{i,j}-1>0$ for $j=3,\dots,n$. $(1/[\lambda_{i,j}])-(3/4)\ge\varpi_{i,j}$ ($j=2,\dots,n$) with $\varpi_{i,j}\ge0$.

Define the overall Lyapunov candidate

$$\begin{aligned} V\quad:=&\sum_{i=1}^{N}V_{i,n}\\ =&\sum_{i=1}^{N}\left[\frac{1}{2}\phi_i^2+\sum_{j=2}^{n}\frac{1}{2}z_{i,j}^2+\sum_{j=2}^{n}\frac{1}{2\sigma_{i,j}}\tilde{W}_{i,j}^{\top}\tilde{W}_{i,j}\right.\\ &+\sum_{j=2}^{n}\frac{1}{3\gamma_{i,j}}|\tilde{\Delta}_{i,j}|^3+\sum_{j=1}^{n}\frac{1}{2\beta_{i,j}}\tilde{\psi}_{i,j}^2+\frac{\rho_i}{2\iota_i}\tilde{\varrho}_i^2\\ &\left.+\frac{1}{2\sigma_{i,1}}\tilde{\theta}_i^2+\frac{\delta_{i,1}}{2\gamma_{i,1}}\tilde{\Delta}_{i,1}^2+\sum_{j=2}^{n}\frac{1}{2}e_{i,j}^2\right]. \end{aligned} \tag{58}$$

Differentiating (58) and using (57), one has

$$\begin{aligned} \dot{V}\le&-\sum_{i=1}^{N}\left[\kappa_{i,1}\phi_i^2+\sum_{j=2}^{n}K_{i,j}z_{i,j}^2+\sum_{j=2}^{n}\varpi_{i,j}e_{i,j}^2\right.\\ &+\frac{1}{2}\sum_{j=1}^{n}\varepsilon_{i,j}\tilde{\psi}_{i,j}^2+\frac{\tau_{i,1}}{2}\tilde{\theta}_{i,1}^2+\frac{\delta_{i,1}\hbar_{i,1}}{2}\tilde{\Delta}_{i,1}^2-\Pi_i\\ &\left.+\frac{1}{2}\sum_{j=2}^{n}(\tau_{i,j}-1)\tilde{W}_{i,j}^{\top}\tilde{W}_{i,j}+\frac{1}{2}\rho_i(\mu_i-\rho_i)\tilde{\varrho}_i^2\right. \end{aligned}$$

$$+\frac{1}{3}\sum_{j=2}^{n}\hbar_{i,j}|\tilde{\Delta}_{i,j}|^3-\sum_{j=1}^{n-1}\Phi_{i,j}^2\Big]. \tag{59}$$

For any $p>0$, we define $\Omega_Z:=\{Z|Z\in\mathbb{R}^{5Nn}, V\le p\}$ with $Z=[\phi_i,\underline{z}_{i,n}^\top,\bar{\tilde{W}}_{i,n}^\top,\underline{\tilde{\Delta}}_{i,n}^\top,\underline{e}_{i,n}^\top,\bar{\tilde{\psi}}_{i,n}^\top,\tilde{\varrho}_i]^\top$, $\underline{z}_{i,n}=[z_{i,2},\ldots,z_{i,n}]^\top$, $\bar{\tilde{W}}_{i,n}=[\tilde{W}_{i,1}^\top,\ldots,\tilde{W}_{i,n}^\top]^\top$, $\underline{\tilde{\Delta}}_{i,n}=[\tilde{\Delta}_{i,2},\ldots,\tilde{\Delta}_{i,n}]^\top$, $\underline{e}_{i,n}=[e_{i,2},\ldots,e_{i,n}]^\top$, $\bar{\tilde{\psi}}_{i,n}=[\tilde{\psi}_{i,1},\ldots,\tilde{\psi}_{i,n}]^\top$. Since $\Phi_{i,j}=\dot{v}_{i,j}$, $v_{i,j}$ are continuous, there exist $\bar{\Phi}_{i,j},\bar{v}_{i,j}>0$, such that $|\Phi_{i,j}|\le\bar{\Phi}_{i,j}$ and $|v_{i,j}|\le\bar{v}_{i,j}$ for $i=1,\ldots,N$, $j=1,\ldots,n-1$, in the compact set $\Omega_Z\times\Omega_d$.

Consider (58) and (59) and choose

$$\begin{aligned}C_1=&\min\{2\kappa_{i,1},2K_{i,j},2\varpi_{i,j},\sigma_{i,1}\tau_{i,1},\sigma_{i,j}(\tau_{i,j}-1),\gamma_{i,j}\hbar_{i,j}\\&\beta_{i,1}\varepsilon_{i,1},\beta_{i,j}\varepsilon_{i,j},\iota_i(\mu_i-\rho_i),\gamma_{i,1}\hbar_{i,1}\},\ \ i=1,\ldots,N\\C_2=&\sum_{i=1}^{N}\left(\Pi_i+\sum_{j=1}^{n-1}\bar{\Phi}_{i,j}^2\right),\ \ j=2,\ldots,n.\end{aligned} \tag{60}$$

Then (61) holds:

$$\dot{V}(t)\le -C_1V(t)+C_2, \tag{61}$$

where $\kappa_{i,1}>0$, $K_{i,j}>0$, $\varpi_{i,j}>0$, $\sigma_{i,1}\tau_{i,1}>0$, $\sigma_{i,j}(\tau_{i,j}-1)>0$, $\gamma_{i,j}\hbar_{i,j}>0$, $\beta_{i,1}\varepsilon_{i,1}>0$, $\beta_{i,j}\varepsilon_{i,j}>0$, $\gamma_{i,1}\hbar_{i,1}>0$ and $\iota_i(\mu_i-\rho_i)>0$. Inequality (61) shows that $\dot{V}<0$ on $V=p$ when $C_1>(C_2/p)$. Consequently, $\Omega_v:=\{V(t)\le p\}$ is an invariant set, implying that $\forall\ t\ge 0$, $V(t)\le p$ holds if $V(0)\le p$. Subsequently, multiplying (61) by e^{C_1t} and integrating it on $[0,t]$, we have

$$V(t)\le V(0)e^{-C_1t}+\frac{C_2}{C_1}\left(1-e^{-C_1t}\right). \tag{62}$$

From (58) and (62), we conclude that the closed-loop signals ϕ_i, $z_{i,j}$, $\tilde{W}_{i,j}$, $\tilde{\Delta}_{i,j}$, $\tilde{\psi}_{i,j}$, $e_{i,j}$ and $\tilde{\varrho}_i$ are SGUUB. According to (10), we have $z_{i,1}=([(\xi_{Hi}-z_{i,1})(\xi_{Li}+z_{i,1})\phi_i]/[\xi_{Hi}\xi_{Li}])$ for $i=1,\ldots,N$, where $\xi_{Hi}>0$, $\xi_{Li}>0$ and $\xi_{Hi}\xi_{Li}>0$. Since ϕ_i are bounded, it follows from (10) that $(\xi_{Hi}-z_{i,1})(\xi_{Li}+z_{i,1})$ are bounded. Therefore, $z_{i,1}$ are bounded. Since the parameters $W_{i,j}^*$, $\Delta_{i,j}$, $\psi_{i,j}$ and ϱ_i, $j=1,\ldots,n$ are bounded, we have $\hat{W}_{i,j}$, $\hat{\Delta}_{i,j}$, $\hat{\psi}_{i,j}$ and $\hat{\varrho}_i$ are bounded. Then, according to (58), the following inequalities hold:

$$\begin{aligned}&0\le\frac{1}{2}\phi_i^2\le V,\quad 0\le\frac{1}{2}z_{i,j}^2\le V,\quad 0\le\frac{1}{2\sigma_{i,j}}\tilde{W}_{i,j}^\top\tilde{W}_{i,j}\le V\\&0\le\frac{1}{2\beta_{i,j}}\tilde{\psi}_{i,j}^2\le V,\quad 0\le\frac{1}{2}e_{i,j}^2\le V\quad 0\le\frac{\rho_i}{2\iota_i}\tilde{\varrho}_i^2\le V\\&0\le\frac{1}{3\gamma_{i,j}}|\tilde{\Delta}_{i,j}|^3\le V,\quad 0\le\frac{\tilde{\theta}_i^2}{2\sigma_{i,1}}\le V,\quad 0\le\frac{\delta_{i,1}\tilde{\Delta}_i^2}{2\gamma_{i,1}}\le V\end{aligned}$$

and, when $t\to\infty$, we have

$$\begin{aligned}&0\le|\phi_i|\le\sqrt{\frac{2C_2}{C_1}},\quad 0\le|z_{i,j}|\le\sqrt{\frac{2C_2}{C_1}}\\&0\le|\tilde{W}_{i,j}|\le\sqrt{\frac{2\sigma_{i,j}C_2}{C_1}},\quad 0\le|\tilde{\Delta}_{i,j}|\le\sqrt[3]{\frac{3\gamma_{i,j}C_2}{C_1}}\\&0\le|\tilde{\psi}_{i,j}|\le\sqrt{\frac{2\beta_{i,j}C_2}{C_1}},\quad 0\le|e_{i,j}|\le\sqrt{\frac{2C_2}{C_1}}\\&0\le|\tilde{\varrho}_i|\le\sqrt{\frac{2\iota_iC_2}{\rho_iC_1}},\quad 0\le|\tilde{\theta}_i|\le\sqrt{\frac{2\sigma_{i,1}C_2}{C_1}}\\&0\le|\tilde{\Delta}_{i,1}|\le\sqrt{\frac{2\gamma_{i,1}C_2}{\delta_{i,1}C_1}}.\end{aligned}$$

Remark 3: From (61) and the Lyapunov practical stability principle, it can be concluded that a larger C_1 leads to faster convergence, while a smaller C_2 can improve the convergence precision. According to (60), the convergence speed and precision of the system errors can be adjusted by tuning the parameters $\kappa_{i,1}$, $K_{i,k}$, $\sigma_{i,j}$, $\tau_{i,j}$, $\gamma_{i,j}$, $\hbar_{i,j}$, $\alpha_{i,j}$, $\beta_{i,j}$, $\varepsilon_{i,j}$, ι_i, and μ_i, where $i=1,\ldots,N$, $j=1,\ldots,n$, and $k=2,\ldots,n$. Specifically, a larger $\kappa_{i,1}$ or $K_{i,k}$ contributes to faster convergence speed. A smaller $\alpha_{i,j}$ improves the precision of system errors. Appropriately chosen parameters $\sigma_{i,j}$, $\tau_{i,j}$, $\gamma_{i,j}$, $\hbar_{i,j}$, $\beta_{i,j}$, $\varepsilon_{i,j}$, ι_i, and μ_i enhance the overall performance of system errors. In practice, designers must carefully balance the tracking performance and control effort. By optimizing these parameters, specific system capacity requirements can be satisfied effectively.

B. Proof of Theorem 1 (b)

It is obvious that within the interval $-\xi_{Li}<z_{i,1}<\xi_{Hi}$ for $i=1,\ldots,N$, using the fact that $0\le|\phi_i|\le\sqrt{(2C_2/C_1)}$, we derive $\{z_{i,1}:=-\zeta_{Li}\le z_{i,1}\le\zeta_{Hi}\}$ with ζ_{Li} and ζ_{Hi} given in (63) and (64).

C. Proof of Theorem 1 (c)

Since both $z_{i,1}$ and y_{di} are bounded, $x_{i,1}$ are also bounded for $i=1,\ldots,N$. From (13), we see that $v_{i,1}$ are bounded. From (6), we obtain that $\hat{v}_{i,2}$ are bounded. Due to the boundedness of signals $z_{i,2}$, $\dot{y}_{di}$, $\hat{v}_{i,2}$, $x_{i,2}$ are also bounded. By induction, it obtains that $v_{i,2},\ldots,v_{i,n-1}$ and $\hat{v}_{i,3},\ldots,\hat{v}_{i,n}$ are all bounded. Then, we get the actual control inputs u_{ci} and system states $x_{i,3},\ldots,x_{i,n}$ are bounded. From (4), the control signals u_i of the actuators are also bounded. Finally, all the signals are SGUUB.

$$\zeta_{Li}=\frac{-[\xi_{Hi}\xi_{Li}+\zeta(\xi_{Hi}-\xi_{Li})]+\sqrt{4\zeta^2\xi_{Hi}\xi_{Li}+(\xi_{Hi}\xi_{Li}+\zeta(\xi_{Hi}-\xi_{Li}))^2}}{2\zeta},\quad \zeta=\sqrt{\frac{2C_2}{C_1}} \tag{63}$$

$$\zeta_{Hi}=\frac{-[\xi_{Hi}\xi_{Li}-\zeta(\xi_{Hi}-\xi_{Li})]+\sqrt{4\zeta^2\xi_{Hi}\xi_{Li}+(\xi_{Hi}\xi_{Li}-\zeta(\xi_{Hi}-\xi_{Li}))^2}}{2\zeta} \tag{64}$$

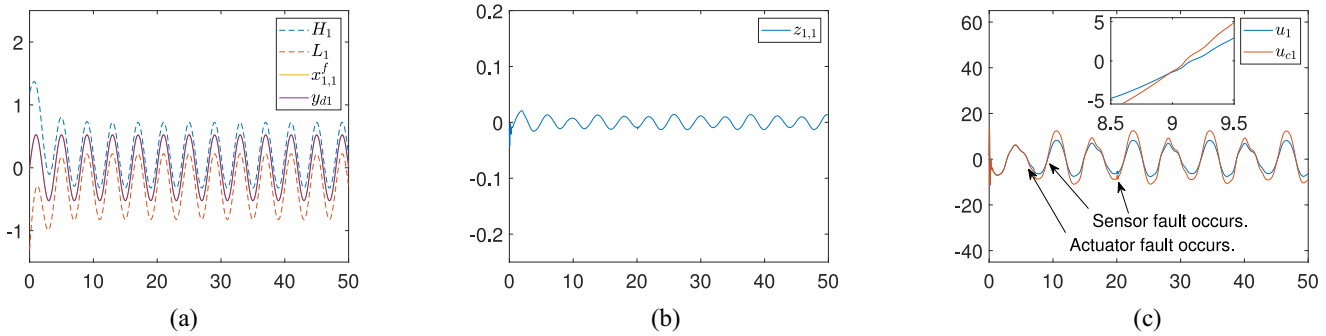

Fig. 2. (a) Reference trajectory y_{d1}, actual trajectory $x^f_{1,1}$, upper bound H_1 and lower bound L_1. (b) Tracking error $z_{1,1}$. (c) Actuator fault input u_1 and actual control input u_{c1}.

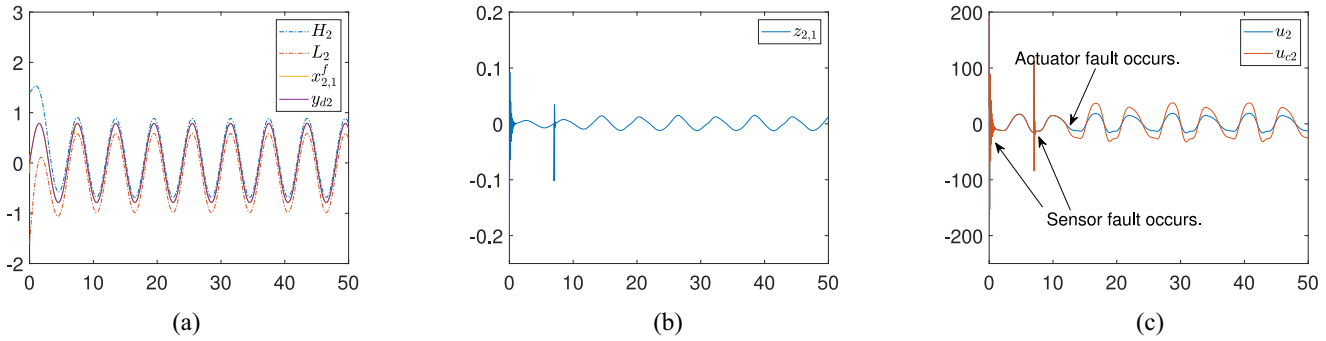

Fig. 3. (a) Reference trajectory y_{d2}, actual trajectory $x^f_{2,1}$, upper bound H_2 and lower bound L_2. (b) Tracking error $z_{2,1}$. (c) Actuator fault input u_2 and actual control input u_{c2}.

D. Proof of Theorem 1 (d)

From $z_{i,1} = x^f_{i,1} - y_{di}$ and Assumption 4, we have $\underline{y}_{di} - \xi_{Li} \leq y_{di} - \xi_{Li} < x^f_{i,1} < \xi_{Hi} + y_{di} \leq \bar{y}_{di} + \xi_{Hi}$. Let $L_i = y_{di} - \xi_{Li}$ and $H_i = y_{di} + \xi_{Hi}$, we have $\underline{y}_{di} - \xi_{Li} \leq L_i < x^f_{i,1} < H_i \leq \bar{y}_{di} + \xi_{Hi}$ for all $t \geq 0$. Therefore, we conclude that the constraints in (2) are satisfied.

V. Simulation Example

Consider two inverted pendulums, connected by a spring and a damper, modelled by [51]

$$\mathcal{J}_1\ddot{\vartheta}_1 = m_1 g r\sin(\vartheta_1) - 0.5\mathcal{F}r\cos(\vartheta_1 - \vartheta) + u_1 + d_1$$
$$\mathcal{J}_2\ddot{\vartheta}_2 = m_2 g r\sin(\vartheta_2) + 0.5\mathcal{F}r\cos(\vartheta_2 - \vartheta) + u_2 + d_2,$$

where $\mathcal{J}_1 = 0.5$ kg $\cdot$ m^2 and $\mathcal{J}_2 = 0.625$ kg $\cdot$ m^2 are the inertia moment, the outputs ϑ_i [rad], $i = 1, 2$ are the pendulums' angles, $m_1 = 2$ kg and $m_2 = 2.5$ kg denote the masses, $g = 9.81$ m/s^2 denotes the gravity acceleration, $\mathcal{F} = k_c(z - l_c) + b_c\dot{z}$ is the spring-damper force applied to the pendulums, $k_c = 150$ N/m and $b_c = 1$ Ns/m are the spring and the damper constants, respectively, $l_c = 0.5$ m represents the natural length, $z = (d_c^2 + rd_c(\sin\vartheta_1 - \sin\vartheta_2) + (r^2/2)(1 + \cos(\vartheta_2 - \vartheta_1)))^{1/2}$ is the current spring length, $r = 0.5$ m is the length, $\vartheta = \arctan(([(r/2)(\cos\vartheta_2 - \cos\vartheta_1)]/[d_c + (r/2)(\sin\vartheta_1 - \sin\vartheta_2)]))$ is the relative angle, $d_c = 0.5$ m is the distance between pendulum base. u_1 and u_2 are the control inputs, and disturbances are $d_1 = 0.1\sin(t)$ and $d_2 = 0.2\cos(t)$. All the initial values and parameters are given in Table III.

TABLE III
Initial Values and Parameters

Initial values	$x_{1,1}(0) = -0.01$, $x_{1,2}(0) = 0.01$, $x_{2,1}(0) = -0.2$, $x_{2,2}(0) = 0.4$, $\hat{\Delta}_{1,1}(0) = \hat{\Delta}_{2,1}(0) = \hat{\Delta}_{1,2}(0) = \hat{\Delta}_{2,2}(0) = 0.1$, $\hat{W}_{1,1}(0) = \hat{W}_{1,2}(0) = \hat{W}_{2,1}(0) = \hat{W}_{2,2}(0) = 0.5(1, \ldots, 1)_{1\times 5}$, $\hat{\varrho}_1(0) = \hat{\varrho}_2(0) = 1$, $\hat{\psi}_{1,1}(0) = \hat{\psi}_{1,2}(0) = \hat{\psi}_{2,1}(0) = \hat{\psi}_{2,2}(0) = 0$.
Design parameters	$\kappa_{1,1} = \kappa_{2,1} = 150$, $\kappa_{1,2} = 50$, $\kappa_{2,2} = 25$, $\sigma_{i,j} = 1$ for $i, j = 1, 2$, $\tau_{1,1} = 0.5$, $\tau_{1,2} = 1.1$, $\tau_{2,1} = 0.8$, $\tau_{2,2} = 1.5$, $\gamma_{1,1} = 6$, $\gamma_{1,2} = 0.1$, $\gamma_{2,1} = 1$, $\gamma_{2,2} = 0.01$, $\hbar_{1,1} = 0.02$, $\hbar_{1,2} = 7$, $\hbar_{2,1} = 0.001$, $\hbar_{2,2} = 2.5$, $\alpha_{1,2} = \alpha_{2,2} = 0.01$, $\lambda_{1,2} = \lambda_{2,2} = 0.1$, $\beta_{1,1} = \beta_{2,1} = 10$, $\beta_{1,2} = \beta_{2,2} = 8$, $\varepsilon_{i,j} = 10$ for $i, j = 1, 2$, $\iota_1 = \iota_2 = 0.1$, $\eta_{1,1} = \eta_{1,2} = 5\exp(-0.01t)$, $\mu_1 = 1.05$, $\mu_2 = 1.01$, $\eta_{2,1} = \eta_{2,2} = \exp(-0.001t)$.

Denote $x_{1,1} = \vartheta_1$, $x_{1,2} = \dot{\vartheta}_1$, $x_{2,1} = \vartheta_2$, and $x_{2,2} = \dot{\vartheta}_2$. The desired trajectories are $y_{d1} = (\pi/6)\sin((\pi/2)t)$, $y_{d2} = (\pi/4)\sin((\pi/3)t)$. The constraint boundaries of $z_{1,1}$, $z_{2,1}$ are $\xi_{H1} = 0.2 + \exp(-0.5t)$, $\xi_{L1} = 0.3 + \exp(-0.6t)$, $\xi_{H2} = 0.1 + 1.3\exp(-0.55t)$, $\xi_{L2} = 0.2 + 1.4\exp(-0.65t)$. The sensor/actuator faults parameters are $\delta_{1,1} = 0.9$, $t^f_{1,1} = 20s$, $\delta_{1,2} = 0.7$, $t^f_{1,2} = 9s$, $\delta_{2,1} = 0.85$, $t^f_{2,1} = 7s$, $\delta_{2,2} = 0.4$, $t^f_{2,2} = 0s$, $\rho_1 = 0.7$, $u_{e1} = 0.5\sin(0.5t)$, $\rho_2 = 0.5$, $u_{e2} = 0.1\sin(t)$, $t^a_1 = 6s$, $t^a_2 = 12s$. The basis functions are $S_k(X_{i,k}) = \exp[-(X_{i,k} - \chi_k)^\top(X_{i,k} - \chi_k)/(2b_k^2)]$, $i = 1, 2$, $k = 1, 2$, where χ_k are random in $(-5, 5)$, and $b_k = \sqrt{2}$. $S_1(X_{i,1})$ contains six nodes, $S_2(X_{i,2})$ contains four nodes, and

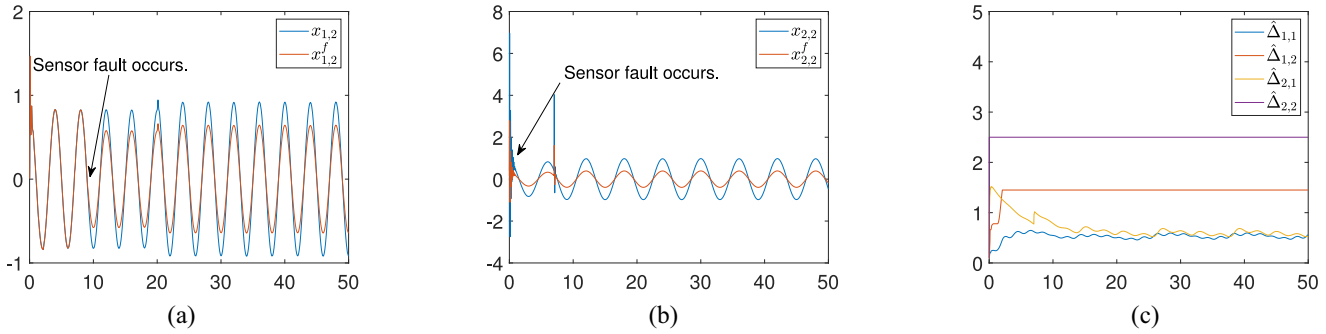

Fig. 4. (a) System state $x_{1,2}$ and sensor measurement value $x^f_{1,2}$. (b) System state $x_{2,2}$ and sensor measurement value $x^f_{2,2}$. (c) Sensor faults adaptive parameters $\hat{\Delta}_{1,1}$, $\hat{\Delta}_{1,2}$, $\hat{\Delta}_{2,1}$ and $\hat{\Delta}_{2,2}$.

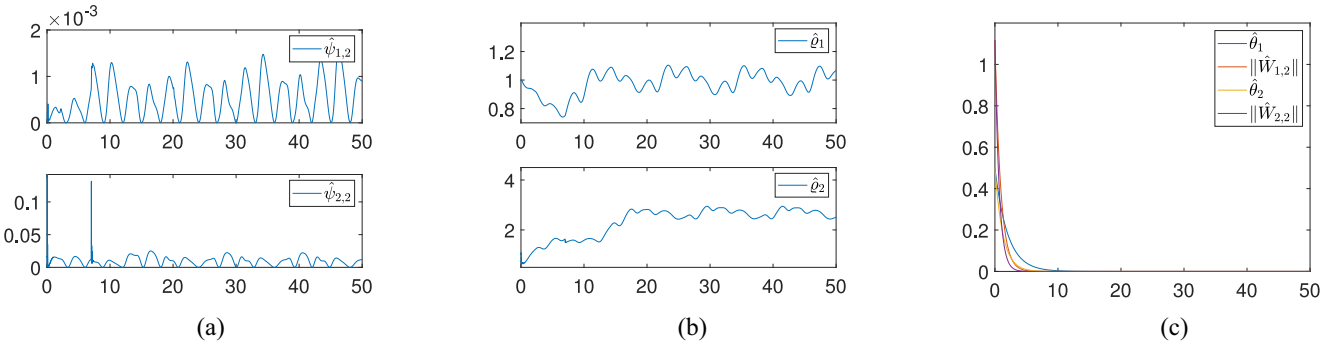

Fig. 5. Actuator faults adaptive parameters. (a) $\hat{\psi}_{1,2}$ and $\hat{\psi}_{2,2}$. (b) $\hat{\varrho}_1$ and $\hat{\varrho}_2$. (c) $\hat{\theta}_1$, $\|\hat{W}_{1,2}\|$, $\hat{\theta}_2$ and $\|\hat{W}_{2,2}\|$.

the inputs of $S_k(X_{i,k})$ are $X_{i,1}=[x^f_{1,1}, x^f_{2,1}, y_{di}, \dot{y}_{di}, \xi_{Hi}, \xi_{Li}]^\top$ and $X_{i,2}=[x^f_{1,1}, x^f_{2,1}, \hat{x}_{1,2}, \hat{x}_{2,2}]^\top$.

Figs. 2–5 illustrate the efficiency of the ANBFTC method. Specifically, the tracking results of $x^f_{1,1}$ and $x^f_{2,1}$are shown in Figs. 2(a) and 3(a) without breaking the output constrains. The boundedness of tracking errors $z_{1,1}$ and $z_{2,1}$ is verified in Figs. 2(b) and 3(b). The boundedness of actuator inputs u_i and actual control inputs u_{ci}, $i = 1, 2$, is shown in Figs. 2(c) and 3(c), which observe that the occurrence of sensor faults causes short-lived fluctuations. Fig. 4(a) and (b) show the response curves of $x_{1,2}$ and $x_{2,2}$, as well as the measured values $x^f_{1,2}$ and $x^f_{2,2}$ with sensor faults, which are all bounded. Figs. 4(c) and 5 show the boundedness of adaptive parameters $\hat{\Delta}_{1,1}$, $\hat{\Delta}_{1,2}$, $\hat{\Delta}_{2,1}$, $\hat{\Delta}_{2,2}$, $\hat{\psi}_{1,2}$, $\hat{\psi}_{2,2}$, $\hat{\varrho}_1$, $\hat{\varrho}_2$, $\hat{\theta}_1$, $\|\hat{W}_{1,2}\|$, $\hat{\theta}_2$, and $\|\hat{W}_{2,2}\|$, respectively.

VI. Conclusion

This article presented a novel ANBFTC control scheme for a class of strict-feedback MIMO nonlinear systems. The backstepping design was implemented through a newly constructed FBACT, and an adaptation strategy was formulated at each iteration step to address unknown disturbances, sensor/actuator faults, and residuals in NN approximation. The faulty sensor measurements, after appropriate adaptive compensation, were utilized as the inputs of RBFNNs. The computational complexity, arising from high-order derivatives of the virtual controller, was mitigated by adopting the DSC technique at each step. Then by integrating BLF into the iterative methodology, the ANBFTC approach was developed for precise output tracking while upholding output constraints. Finally, we demonstrated the effectiveness of the ANBFTC approach through a simulation example. Future works will focus on exploring sensor/actuator failures in MIMO nonlinear systems.

References

[1] Y.-X. Li, "Command filter adaptive asymptotic tracking of uncertain nonlinear systems with time-varying parameters and disturbances," *IEEE Trans. Autom. Control*, vol. 67, no. 6, pp. 2973–2980, Jun. 2022.

[2] S. Lu, M. Chen, Y. Liu, and S. Shao, "Adaptive NN tracking control for uncertain MIMO nonlinear system with time-varying state constraints and disturbances," *IEEE Trans. Neural Netw. Learn. Syst.*, vol. 34, no. 10, pp. 7309–7323, Oct. 2023.

[3] J. Ma, J. H. Park, and S. Xu, "Global adaptive control for uncertain nonlinear systems with sensor and actuator faults," *IEEE Trans. Syst., Man, Cybern., Syst.*, vol. 51, no. 9, pp. 5503–5510, Sep. 2021.

[4] Y.-J. Liu and S. Tong, "Barrier Lyapunov functions-based adaptive control for a class of nonlinear pure-feedback systems with full state constraints," *Automatica*, vol. 64, pp. 70–75, Feb. 2016.

[5] N. Zhou, X. Cheng, Z. Sun, and Y. Xia, "Fixed-time cooperative behavioral control for networked autonomous agents with second-order nonlinear dynamics," *IEEE Trans. Cybern.*, vol. 52, no. 9, pp. 9504–9518, Sep. 2022.

[6] E. Kayacan, E. Kayacan, H. Ramon, and W. Saeys, "Towards agrobots: Identification of the yaw dynamics and trajectory tracking of an autonomous tractor," *Comput. Electron. Agricult.*, vol. 115, pp. 78–87, Jul. 2015.

[7] W. Xie, D. Cabecinhas, R. Cunha, and C. Silvestre, "Adaptive backstepping control of a quadcopter with uncertain vehicle mass, moment of inertia, and disturbances," *IEEE Trans. Ind. Electron.*, vol. 69, no. 1, pp. 549–559, Jan. 2022.

[8] M. Arteaga and B. Siciliano, "On tracking control of flexible robot arms," *IEEE Trans. Autom. Control*, vol. 45, no. 3, pp. 520–527, Mar. 2000.

[9] G. Wen, S. S. Ge, C. L. P. Chen, F. Tu, and S. Wang, "Adaptive tracking control of surface vessel using optimized backstepping technique," *IEEE Trans. Cybern.*, vol. 49, no. 9, pp. 3420–3431, Sep. 2019.

[10] P. K. Mishra, N. K. Dhar, and N. K. Verma, "Adaptive neural-network control of MIMO nonaffine nonlinear systems with asymmetric time-varying state constraints," *IEEE Trans. Cybern.*, vol. 51, no. 4, pp. 2042–2054, Apr. 2021.

[11] X. Jin, "Adaptive fixed-time control for MIMO nonlinear systems with asymmetric output constraints using universal barrier functions," *IEEE Trans. Autom. Control*, vol. 64, no. 7, pp. 3046–3053, Jul. 2019.

[12] D. Li, L. Liu, Y.-J. Liu, S. Tong, and C. L. P. Chen, "Adaptive NN control without feasibility conditions for nonlinear state constrained stochastic systems with unknown time delays," *IEEE Trans. Cybern.*, vol. 49, no. 12, pp. 4485–4494, Dec. 2019.

[13] D. Li, H.-G. Han, and J.-F. Qiao, "Composite boundary structure-based tracking control for nonlinear state-dependent constrained systems," *IEEE Trans. Autom. Control*, vol. 69, no. 8, pp. 5686–5693, Aug. 2024.

[14] Y. Song, Y. Wang, and C. Wen, "Adaptive fault-tolerant PI tracking control with guaranteed transient and steady-state performance," *IEEE Trans. Autom. Control*, vol. 62, no. 1, pp. 481–487, Jan. 2017.

[15] N. Zhou, Y. Kawano, and M. Cao, "Neural network-based adaptive control for spacecraft under actuator failures and input saturations," *IEEE Trans. Neural Netw. Learn. Syst.*, vol. 31, no. 9, pp. 3696–3710, Sep. 2020.

[16] J. Zhang, S.-C. Tong, and Y.-M. Li, "Adaptive fuzzy finite-time output-feedback fault-tolerant control of nonstrict-feedback systems against actuator faults," *IEEE Trans. Syst., Man, Cybern., Syst.*, vol. 52, no. 2, pp. 1276–1287, Feb. 2022.

[17] Z. Zhang, Y. Dong, and G. Duan, "Global asymptotic fault-tolerant tracking for time-varying nonlinear complex systems with prescribed performance," *Automatica*, vol. 159, Jan. 2024, Art. no. 111345.

[18] S. Zhou and Y. Song, "Prescribed performance neuroadaptive fault-tolerant compensation for MIMO nonlinear systems under extreme actuator failures," *IEEE Trans. Syst., Man, Cybern., Syst.*, vol. 51, no. 9, pp. 5427–5436, Sep. 2021.

[19] J. Liu and J. Dong, "Distributed fault-tolerant control for nonlinear heterogeneous multiagent system with fault indication under safety constraint," *IEEE Trans. Syst., Man, Cybern., Syst.*, vol. 54, no. 6, pp. 3843–3853, Jun. 2024.

[20] F. Jia and X. He, "Fault-tolerant control for uncertain nonstrict-feedback stochastic nonlinear systems with output constraints," *IEEE Trans. Syst., Man, Cybern., Syst.*, vol. 53, no. 8, pp. 5212–5223, Aug. 2023.

[21] Y.-X. Li and G.-H. Yang, "Adaptive asymptotic tracking control of uncertain nonlinear systems with input quantization and actuator faults," *Automatica*, vol. 72, pp. 177–185, Oct. 2016.

[22] Z. Ruan, Q. Yang, S. S. Ge, and Y. Sun, "Adaptive fuzzy fault tolerant control of uncertain MIMO nonlinear systems with output constraints and unknown control directions," *IEEE Trans. Fuzzy Syst.*, vol. 30, no. 5, pp. 1224–1238, May 2022.

[23] Z. Han, Z. Liu, J.-W. Wang, and W. He, "Fault-tolerant control for flexible structures with partial output constraint," *IEEE Trans. Autom. Control*, vol. 69, no. 4, pp. 2668–2675, Apr. 2024.

[24] S. Zeghlache, H. Rahali, A. Djerioui, L. Benyettou, and M. F. Benkhoris, "Robust adaptive backstepping neural networks fault tolerant control for mobile manipulator UAV with multiple uncertainties," *Math. Comput. Simul.*, vol. 218, pp. 556–585, Apr. 2024.

[25] H. Gao, Y. Song, and C. Wen, "Backstepping design of adaptive neural fault-tolerant control for MIMO nonlinear systems," *IEEE Trans. Neural Netw. Learn. Syst.*, vol. 28, no. 11, pp. 2605–2613, Nov. 2017.

[26] X. Cao, P. Shi, Z. Li, and M. Liu, "Neural-network-based adaptive backstepping control with application to spacecraft attitude regulation," *IEEE Trans. Neural Netw. Learn. Syst.*, vol. 29, no. 9, pp. 4303–4313, Sep. 2018.

[27] J.-X. Zhang and G.-H. Yang, "Fault-tolerant output-constrained control of unknown Euler–Lagrange systems with prescribed tracking accuracy," *Automatica*, vol. 111, Jan. 2020, Art. no. 108606.

[28] X. Jin, "Adaptive fault tolerant tracking control for a class of stochastic nonlinear systems with output constraint and actuator faults," *Syst. Control Lett.*, vol. 107, pp. 100–109, Sep. 2017.

[29] L. Ma, Z. Wang, H. Zhang, and Q. Wang, "Adaptive neural network constrained fault tolerant control for nonlinear systems with actuator failures and saturation," *IEEE Trans. Autom. Sci. Eng.*, early access, May 29, 2024, doi: 10.1109/TASE.2024.3381780.

[30] N. Zhou, X. Cheng, Y. Xia, and Y. Liu, "Fully adaptive-gain-based intelligent failure-tolerant control for spacecraft attitude stabilization under actuator saturation," *IEEE Trans. Cybern.*, vol. 52, no. 1, pp. 344–356, Jan. 2022.

[31] J. Wang, J. Ma, H. Pan, and W. Sun, "Event-triggered adaptive saturated fault-tolerant control for unknown nonlinear systems with full state constraints," *IEEE Trans. Autom. Sci. Eng.*, vol. 21, no. 2, pp. 1837–1849, Apr. 2024.

[32] Y. Zheng and Y.-X. Li, "Event-triggered output feedback consensus tracking control for nonlinear multiagent systems with sensor failures," *Automatica*, vol. 148, Feb. 2023, Art. no. 110787.

[33] C. Sun and Y. Lin, "Adaptive output feedback compensation for a class of nonlinear systems with actuator and sensor failures," *IEEE Trans. Syst., Man, Cybern., Syst.*, vol. 52, no. 8, pp. 4762–4771, Aug. 2022.

[34] Z. Zhang, C. Wen, Y. Song, and G. Feng, "Adaptive quantized output feedback control of nonlinear systems with mismatched uncertainties and sensor failures," *IEEE Trans. Autom. Control*, vol. 62, no. 12, pp. 8216–8223, Dec. 2023.

[35] H. Habibi, A. Yazdani, M. Darouach, H. Wang, T. Fernando, and I. Howard, "Observer-based sensor fault-tolerant control with prescribed tracking performance for a class of nonlinear systems," *IEEE Trans. Autom. Control*, vol. 68, no. 12, pp. 8259–8266, Dec. 2023.

[36] X. Zhang, "Sensor bias fault detection and isolation in a class of nonlinear uncertain systems using adaptive estimation," *IEEE Trans. Autom. Control*, vol. 56, no. 5, pp. 1220–1226, May 2011.

[37] L. Cao, H. Li, G. Dong, and R. Lu, "Event-triggered control for multiagent systems with sensor faults and input saturation," *IEEE Trans. Syst., Man, Cybern., Syst.*, vol. 51, no. 6, pp. 3855–3866, Jun. 2021.

[38] Y. Song, B. Zhang, and K. Zhao, "Indirect neuroadaptive control of unknown MIMO systems tracking uncertain target under sensor failures," *Automatica*, vol. 77, pp. 103–111, Mar. 2017.

[39] X. Huang, C. Wen, and Y. Song, "Adaptive neural control for uncertain constrained pure feedback systems with severe sensor faults: A complexity reduced approach," *Automatica*, vol. 147, Jan. 2023, Art. no. 110701.

[40] R. Meng, C. Hua, K. Li, and P. Ning, "General output constraints control of interconnected nonlinear systems with sensor faults," *J. J. Franklin Inst.*, vol. 361, no. 17, 2024, Art. no. 107178.

[41] Y. Liu, Z. Chen, L. Wei, X. Wang, and L. Li, "Braking sensor and actuator fault diagnosis with combined model-based and data-driven pressure estimation methods," *IEEE Trans. Ind. Electron.*, vol. 70, no. 11, pp. 11639–11648, Nov. 2023.

[42] K. Li, S. X. Ding, W. X. Zheng, and C.-C. Hua, "Global distributed fault-tolerant consensus control of nonlinear delayed multiagent systems with hybrid faults," *IEEE Trans. Autom. Control*, vol. 69, no. 3, pp. 1967–1974, Mar. 2024.

[43] D. Yu, M. Yang, Y.-J. Liu, Z. Wang, and C. L. P. Chen, "Adaptive fuzzy tracking control for uncertain nonlinear systems with multiple actuators and sensors faults," *IEEE Trans. Fuzzy Syst.*, vol. 31, no. 1, pp. 104–116, Jan. 2023.

[44] H. Wang, J. Ma, X. Zhao, B. Niu, M. Chen, and W. Wang, "Adaptive fuzzy fixed-time control for high-order nonlinear systems with sensor and actuator faults," *IEEE Trans. Fuzzy Syst.*, vol. 31, no. 8, pp. 2658–2668, Aug. 2023.

[45] Y. Wu, J. Liu, Z. Wang, and Z. Ju, "Distributed resilient tracking of multiagent systems under actuator and sensor faults," *IEEE Trans. Cybern.*, vol. 53, no. 7, pp. 4653–4664, Jul. 2023.

[46] T. Yang and J. Dong, "Funnel-based predefined-time containment control of heterogeneous multiagent systems with sensor and actuator faults," *IEEE Trans. Syst., Man, Cybern., Syst.*, vol. 54, no. 3, pp. 1903–1913, Mar. 2024.

[47] D. Li, H.-G. Han, and J.-F. Qiao, "Fuzzy-approximation adaptive fault tolerant control for nonlinear constraint systems with actuator and sensor faults," *IEEE Trans. Fuzzy Syst.*, vol. 32, no. 5, pp. 2614–2624, May 2024.

[48] J. Wang, H. Pan, and W. Sun, "Event-triggered adaptive output constraint tracking control of uncertain MIMO nonlinear systems with sensor and actuator faults," *IEEE Trans. Autom. Sci. Eng.*, vol. 21, no. 4, pp. 6774–6786, Oct. 2024.

[49] D. Swaroop, J. Hedrick, P. P. Yip, and J. Gerdes, "Dynamic surface control for a class of nonlinear systems," *IEEE Trans. Autom. Control*, vol. 45, no. 10, pp. 1893–1899, Oct. 2000.

[50] L. Kong, W. He, Z. Liu, X. Yu, and C. Silvestre, "Adaptive tracking control with global performance for output-constrained MIMO nonlinear systems," *IEEE Trans. Autom. Control*, vol. 68, no. 6, pp. 3760–3767, Jun. 2023.

[51] F. Fotiadis and G. A. Rovithakis, "Input-constrained prescribed performance control for high-order MIMO uncertain nonlinear systems via reference modification," *IEEE Trans. Autom. Control*, vol. 69, no. 5, pp. 3301–3308, May 2024.

Ning Zhou (Member, IEEE) received the M.S. degree in applied mathematics from the Liaoning University of Technology, Jinzhou, China, in 2011, and the Ph.D. degree in control science and engineering from the Beijing Institute of Technology, Beijing, China, in 2015.

She was a Postdoctoral Scholar with the Faculty of Science and Engineering, University of Groningen, Groningen, The Netherlands, from 2017 to 2019. She was a Lecturer with the College of Computer and Information Sciences, Fujian Agriculture and Forestry University, Fuzhou, China, from 2015 to 2019. She is currently an Associate Professor with the School of Electrical Engineering, Hebei University of Science and Technology, Shijiazhuang, China. Her main research interests include spacecraft attitude synchronization, sliding mode control, fault-tolerant control, intelligent control, and cooperative control.

Canyang Zhao was born in Shijiazhuang, China. He received the B.S. degree in electrical engineering and automation from Shijiazhuang University, Shijiazhuang, Hebei, China, in 2022. He is currently pursuing the M.S. degree in electronic information with Hebei University of Science and Technology, Shijiazhuang.

His current research interests include nonlinear systems, backstepping control, adaptive neural (NN) control, time-varying output constraints control, and fault-tolerant control.

Xiaodong Cheng (Senior Member, IEEE) received the B.Sc. and M.Sc. degrees in system engineering from Northwestern Polytechnical University, Xi'an, China, in 2011 and 2014, respectively, and the Ph.D. degree in systems and control from the University of Groningen, Groningen, The Netherlands, in 2018.

He is an Assistant Professor with the Mathematical and Statistical Methods Group (Biometris), Wageningen University and Research, Wageningen, The Netherlands. From 2019 to 2022, he was a Postdoctoral Researcher with the Eindhoven University of Technology, Eindhoven, The Netherlands, and then a Research Associate with the Department of Engineering, the University of Cambridge, Cambridge, U.K. His main research interests include system identification, model reduction, and control applications in energy systems and agriculture.

Dr. Cheng is the recipient of the Paper Prize Award from the IFAC Journal Automatica in the triennium from 2017 to 2019, and the Outstanding Paper Award from IEEE Transactions on Control Systems Technology in 2020.

Yuanqing Xia (Fellow, IEEE) received the Ph.D. degree in control theory and control engineering from Beihang University, Beijing, China, in 2001.

He was a Research Fellow in several academic institutions from 2002 to 2008, including the National University of Singapore, Singapore, and the University of Glamorgan, Newport, U.K. Since 2004, he has been with the Beijing Institute of Technology, Beijing, where he is currently a Full Professor. He is also the President of the Zhongyuan University of Technology, Zhengzhou, China. He obtained the National Outstanding Youth Foundation of China in 2012, and was honored as a Yangtze River Scholar Distinguished Professor in 2016. His research interests include cloud control systems, networked control systems, signal processing, active disturbance rejection control, unmanned system control, and flight control.